

MICROCOPY RESOLUTION TEST CHART
NATIONAL BUREAU OF STANDARDS-1963-A

12

AD A127541

CONTRACT NO. N00019-80-C-0575

ATC REPORT NO. R-92000/2CR-20

**Roll-Bonded 300M/1010 Steel Metal-Metal Laminates:
Forgeability, Toughness, Fatigue, and Stress Corrosion**

L. E. SLOTER

VOUGHT CORPORATION ADVANCED TECHNOLOGY CENTER

P. O. BOX 226144
DALLAS, TEXAS 75266

JUNE 1982

FINAL REPORT FOR PERIOD SEPTEMBER 1980 - DECEMBER 1981

APPROVED FOR PUBLIC RELEASE; DISTRIBUTION UNLIMITED

Prepared for:

DEPARTMENT OF THE NAVY
NAVAL AIR SYSTEMS COMMAND
WASHINGTON, D. C. 20361

DTIC FILE COPY

DTIC
ELECTE
MAY 02 1983
S D
E

 **VOUGHT CORPORATION**
Advanced Technology Center

83 05 02 01Z

UNCLASSIFIED

SECURITY CLASSIFICATION OF THIS PAGE (When Data Entered)

REPORT DOCUMENTATION PAGE		READ INSTRUCTIONS BEFORE COMPLETING FORM
1. REPORT NUMBER	2. GOVT ACCESSION NO. AD-A127541	3. RECIPIENT'S CATALOG NUMBER
4. TITLE (and Subtitle) Roll-Bonded 300M/1010 Steel Metal-Metal Laminates: Forgeability, Toughness, Fatigue, and Stress Corrosion		5. TYPE OF REPORT & PERIOD COVERED Final Report for Period 18 Sept 1980 - 18 Dec 1981
7. AUTHOR(s) L. E. Sloter		6. PERFORMING ORG. REPORT NUMBER R-92000/2CR-20
9. PERFORMING ORGANIZATION NAME AND ADDRESS Vought Corporation Advanced Technology Center P.O. Box 226144 Dallas, Texas 75266		8. CONTRACT OR GRANT NUMBER(s) N00019-80-C-0575
11. CONTROLLING OFFICE NAME AND ADDRESS Department of the Navy Naval Air Systems Command Washington D. C. 20361		10. PROGRAM ELEMENT, PROJECT, TASK AREA & WORK UNIT NUMBERS
14. MONITORING AGENCY NAME & ADDRESS (if different from Controlling Office)		12. REPORT DATE June, 1982
		13. NUMBER OF PAGES 97
		15. SECURITY CLASS. (of this report) UNCLASSIFIED
		15a. DECLASSIFICATION/DOWNGRADING SCHEDULE
16. DISTRIBUTION STATEMENT (of this Report) Approved for public release; distribution unlimited		
17. DISTRIBUTION STATEMENT (of the abstract entered in Block 20, if different from Report)		
18. SUPPLEMENTARY NOTES		
19. KEY WORDS (Continue on reverse side if necessary and identify by block number) Alloy 300M, Fatigue Strength, Forgeability, Forging, Fracture Toughness; K _{ISCC} , Laminates, Metal Laminates, Plastic Buckling, Roll Bonding, Steel, Stress Corrosion Cracking		
20. ABSTRACT (Continue on reverse side if necessary and identify by block number) The fabrication of Alloy 300M/1010 steel metal-metal laminates in thick section by hot roll bonding is described and discussed. The results of the forgeability testing of the roll-bonded laminate plate and the tensile, fracture toughness, fatigue, and stress-corrosion cracking properties of the roll-bonded and roll-bonded and forged laminate material and 300M monolithic control material are reported, evaluated, and discussed. Two thick laminate billets in which eighteen layers of 300M low alloy steel separated by seventeen inter-leaves of 1010 mild steel have been prepared by hot roll bonding from plate		

DD FORM 1473

1 JAN 73

EDITION OF 1 NOV 68 IS OBSOLETE

S/N 0102-LF-014-6601

UNCLASSIFIED

SECURITY CLASSIFICATION OF THIS PAGE (When Data Entered)

UNCLASSIFIED

SECURITY CLASSIFICATION OF THIS PAGE (When Data Entered)

and sheet stock. Cylindrical specimens machined from these billets have been forged in both open and closed dies and the laminate forgeability established. The forgeability of the laminate in the longitudinal direction, i.e., material flow perpendicular to the lamellar plane, is limited to low strains, less than -27%, by the hot strength of the interlamellar bonds and the plastic buckling resistance of the laminate. The forgeability in the transverse direction, i.e., material flow parallel to the lamellar plane, is limited only by the acceptable reorientation of laminate fiber caused by die shape and the frictional characteristics of the process, the transverse flow of the layers and interleaves being completely stable in the 300M/1010 system. The effects of forging on the mechanical properties of the laminate primarily result from the decreased layer thicknesses and improved bond integrity that obtain with flow. Improved fracture toughness results from the decreased layer thickness up to a maximum at which the improved bond integrity begins to degrade the ability of the layers to fracture independently. An improvement in toughness of 300 percent over monolithic 300M is evinced by a forged laminate. The tensile strength of the laminate is decreased with respect to monolithic 300M by the volume fraction of low strength mild steel in the laminate and by the plastic constraint imposed on the layers by the interleaves during tensile elongation. Tensile strengths for the laminate materials were above 200 ksi (1379 MPa) versus 263 ksi (1813 MPa) for the monolithic 300M. The laminate uniform elongation and tensile elongation are superior to the monolithic material. In high cycle fatigue tests the superior damage tolerance of the roll-bonded laminate results in improved fatigue strength at least 10⁷ cycles. Finally, the stress intensity factor for stress-corrosion cracking, K_{Isc} , in simulated sea water is significantly increased in the roll-bonded laminate system versus monolithic 300M, being 32 ksi-in^{1/2} versus 15 ksi - in^{1/2} (35 versus 17 MPa - m^{1/2}). The stress-corrosion crack propagation rates at high stress intensities are approximately equal in the laminate and monolithic systems.

S/N 0102-LF-014-6601

UNCLASSIFIED

SECURITY CLASSIFICATION OF THIS PAGE (When Data Entered)

PREFACE

This report is a description of the procedures and results of the "Forged Laminates for Structures Study" conducted at the Vought Corporation Advanced Technology Center during the period 18 September 1980 through 18 November 1981. The study was conducted for the Naval Air Systems Command under Contract N00019-80-C-0575. The contract monitors for the study were Mr. Michael Valentine and Mr. Joseph Bruce, Naval Air Systems Command, Codes AIR-5304B4 and AIR-5304B5, respectively.

The study was conducted under the supervision of Dr. D. H. Petersen, Manager - Structures and Materials Research; the Principal Investigator was Dr. L. E. Sloter. Commendable technical support was provided by Messrs. J. H. Thomas, F. H. Ebel, B. K. Austin, and C. P. Robinson. Additional technical support was provided by Dr. L. J. Cuddy and Messrs. R. C. Adams and J. C. Raley of the United States Steel Research Laboratories, Monroeville, Pennsylvania, in the roll bonding of the steel laminates, by Dr. S. C. Jain of the Beaumont Well Works Company, Houston, Texas, in the open die forging of the laminate, and by Messrs. W. E. Latta, P. G. Evers, J. Pillar, D. Leitgeb, T. Bain, and T. Egnot of Pittsburgh Forgings Company, Corapolois, Pennsylvania, who were all extremely helpful in the arrangement and performance of the closed die forging of the laminate material on standard production equipment. In addition to the technical suggestions of Messrs. Bruce and Valentine, the interest shown and the suggestions contributed by Mr. R. Schmidt, Code AIR-320, and Mr. J. F. Collins, Code AIR-5304B, have been very valuable to the nature and content of the study.

Accession For	
NTIS GRA&I	<input checked="" type="checkbox"/>
DTIC TAB	<input type="checkbox"/>
Unannounced	<input type="checkbox"/>
Justification	
By	
Distribution/	
Availability Codes	
Dist	Avail and/or Special
A	



TABLE OF CONTENTS

	PAGE NO.
PREFACE	
1.0 INTRODUCTION	1
2.0 EXPERIMENTAL PROCEDURE	10
2.1 MATERIAL SELECTION	10
2.2 LAMINATE PREPARATION	10
2.3 FORGEABILITY TESTING	13
2.4 COMPLEX FLOW EVALUATION	15
2.5 PHYSICAL EVALUATION	17
2.6 HEAT TREATMENT	20
2.7 MECHANICAL TESTING	20
2.7.1 Tensile Properties	20
2.7.2 Fracture Properties	20
2.7.3 Fatigue Strength	23
2.8 STRESS-CORROSION CRACKING EVALUATION	23
3.0 RESULTS AND DISCUSSION	24
3.1 LAMINATE PREPARATION	24
3.1.1 Laminate Micrography	24
3.2 FORGEABILITY TESTING	26
3.2.1 Tensile Properties	41
3.2.2 Micrography	45
3.3.3 Fracture Properties	49
3.3 COMPLEX FLOW EVALUATION (CLOSED DIE FORGING)	56
3.3.1 Micrography	58
3.3.2 Tensile Properties	62
3.3.3 Fracture Properties	65
3.4 GENERAL DISCUSSION OF LAMINATE FRACTURE TOUGHNESS	68
3.5 GENERAL DISCUSSION OF MATERIAL FLOW AND FRACTURE TOUGHNESS	72
3.6 FATIGUE STRENGTH OF ROLL-BONDED LAMINATES	75
3.7 STRESS-CORROSION CRACKING OF ROLL-BONDED LAMINATES	80
4.0 CONCLUSIONS	85
5.0 RECOMMENDATIONS	87
REFERENCES	88
DISTRIBUTION LIST	

1.0 INTRODUCTION

The practice of utilizing layers of dissimilar materials in order to achieve desired properties in structures and other useful items originated during prehistory. By the time the early Middle Eastern and Oriental civilizations were firmly established the exploitation of layered materials for both aesthetic purposes, such as wood veneer and gilding, and structural purposes, such as the banding of wood with metal, already had become quite sophisticated.¹ During the past several decades the application of highly advanced laminar composites has been effected, particularly in the aerospace industry. Such laminated composites offer the potential for improved reliability, durability, and damage tolerance combined with lower maintenance requirements and life cycle costs when compared with conventionally wrought and machined items. Other appealing properties of laminates are the high specific moduli and strength characteristics and higher fracture and fatigue resistance potentially achievable through proper laminae and lamination process selection. In particular, the enhancement of fracture toughness and fatigue resistance through lamination has been the subject of intense investigation.²⁻²⁸ Laminates investigated have included single constituents bonded together²⁻²⁵ and duplex or multiplex laminates formed by a variety of techniques.²⁶⁻³⁶ Although these studies have shown that lamination is beneficial for fatigue and fracture resistance, only the investigations of Ohlson¹⁹ and Goolsby⁴ have provided a thorough evaluation of lamina and laminate thickness effects on fracture toughness, using current fracture toughness testing procedures. In particular, the early work⁴ conducted at the Vought Advanced Technology Center has shown that laminate toughness can be maximized by proper selection of lamina material and thickness.

Metal laminates are a type of laminar composite and typically consist of multilayers of bonded homogeneous laminae as shown in Figure 1. Although the layers are generally of a single homogeneous material, each layer may be isotropic, orthotropic, or anisotropic depending on material properties, such as the basic crystalline structure and texture. The type of bonding provides a convenient classification of laminar composites, the two basic bonding techniques employed involving either a direct metal-to-metal (metallurgical) bond or

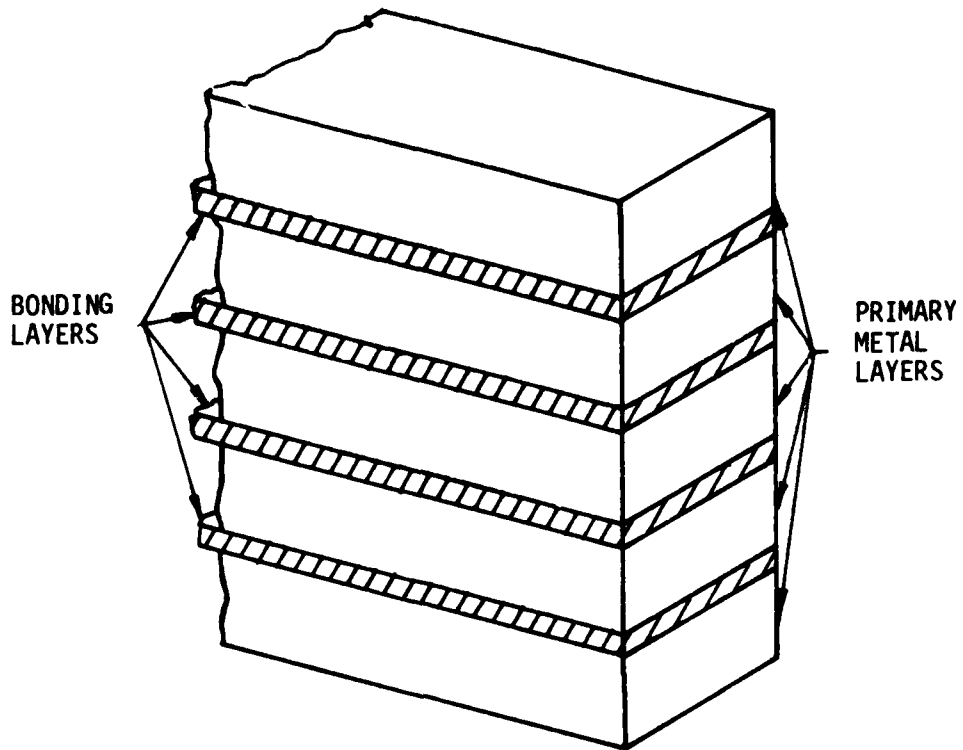


FIGURE 1. SCHEMATIC METAL LAMINATE.

an adhesive bond, such as that produced by an epoxy adhesive layer. Bonding with adhesives is a relatively easy low temperature process that provides the necessary conditions for high fracture toughness. Metal-to-metal bonding typically is achieved by diffusion bonding, brazing, soldering, roll bonding, or explosion bonding and may or may not provide the necessary delamination conditions required for high fracture toughness.

Previous investigations^{4,33-36} performed at the Vought Corporation Advanced Technology Center (ATC) have established that significant benefits are derivable through the use of metal-metal laminates. These laminate materials offer high toughness, crack arrest capacity, and subcritical crack growth resistance. The ATC Metal Laminates for Structures Program has demonstrated these beneficial capacities in plate materials formed by explosion bonding, diffusion bonding, and roll bonding. In particular, roll-bonded metal-metal laminate plates composed of layers of high strength metal alloys and interleaved with dissimilar lower strength alloys (Figure 2) have been shown to have thick section tensile and fracture toughness properties that are superior to a corresponding section of monolithic or unlaminated alloys. These superior properties derive from both the crack dividing and the crack arresting properties of the generally softer interleaf alloy. Since the crack arrest and crack divider orientations are of importance in orienting laminate fracture properties and laminar composite application, they are illustrated in Figure 3. Mechanistically in the crack divider orientation, the controlled delamination of the layers during the fast fracture of thick laminates results in a plane or nearly plane stress rather than a plane strain fracture, and, therefore, the energy required for fracture or the fracture toughness is greatly increased. This rationale is illustrated schematically in Figure 4 in which the general inverse relationship of fracture toughness versus thickness is contrasted with laminate behavior. As shown in the figure, the toughness of most materials decreases from a plane stress maximum at thin section sizes through a mixed stress region to a pure plane strain limiting value that may be defined as the plane strain fracture toughness.³⁷ In the crack arrest orientation, the interleaf effectively blunts a running crack by plastic flow in the case of a soft interleaf or interfacial separation, thereby slowing or stopping the crack and concomitantly improving the fracture toughness. Moreover, laminates may be fabricated to provide other enhanced properties, such

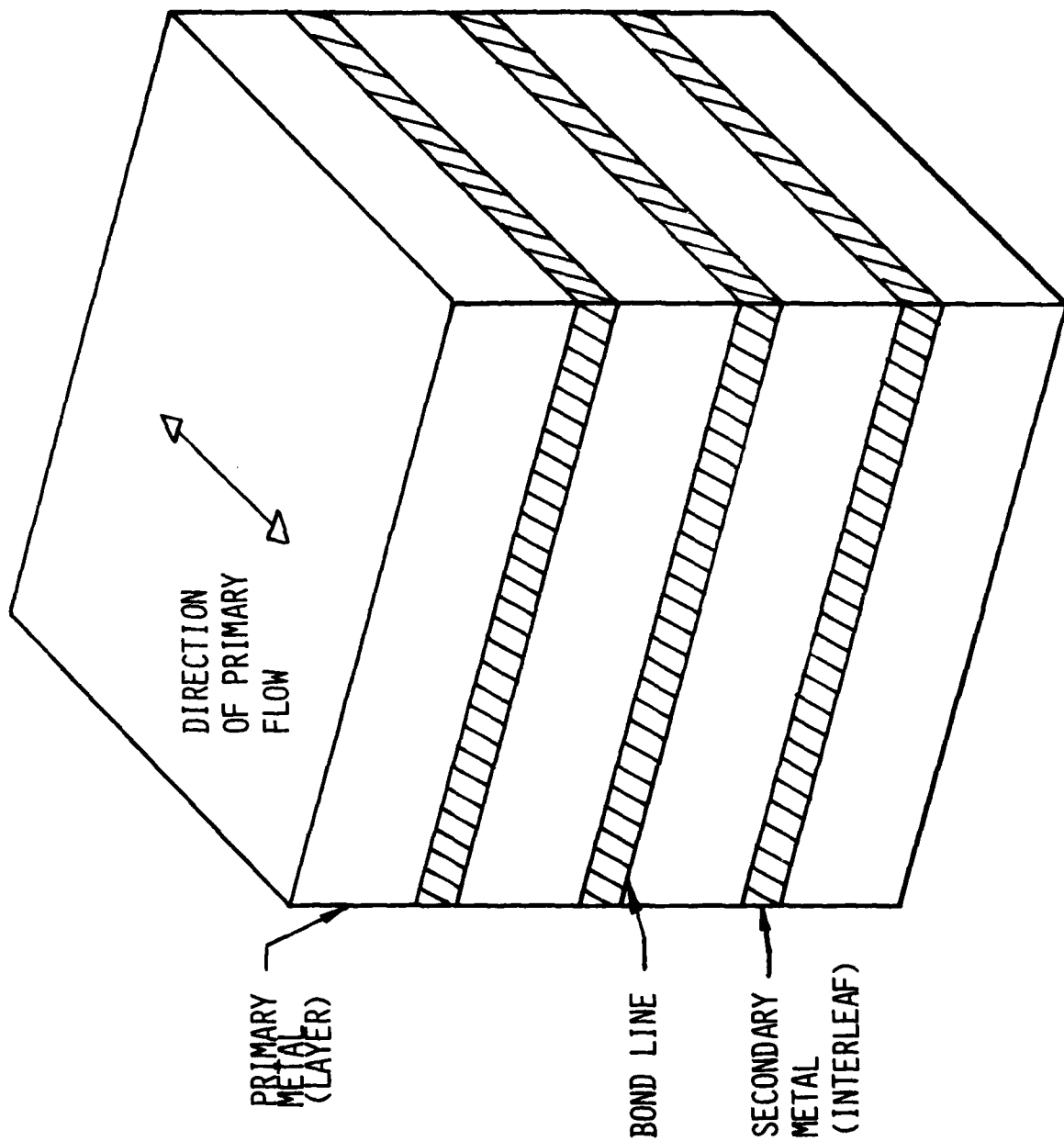
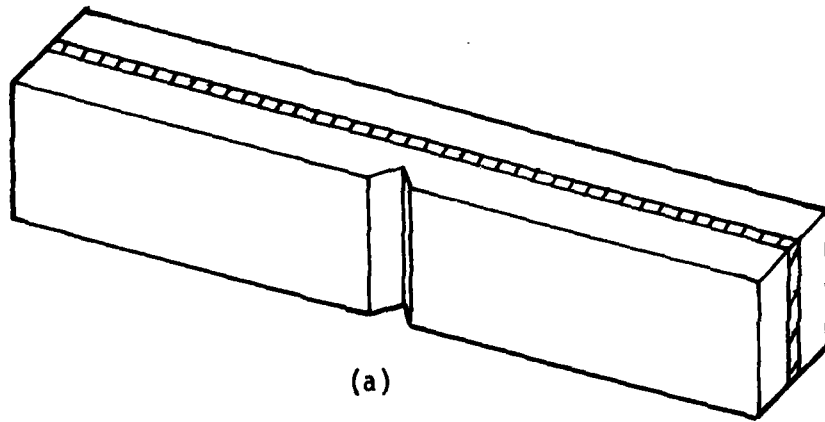
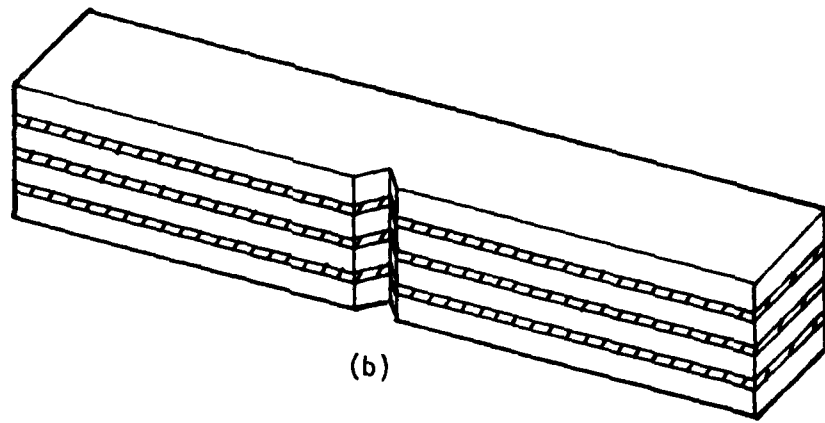


FIGURE 2. SCHEMATIC METAL-METAL LAMINATE.



(a)



(b)

FIGURE 3. (a) CRACK ARREST AND (b) CRACK DIVIDER ORIENTATIONS.

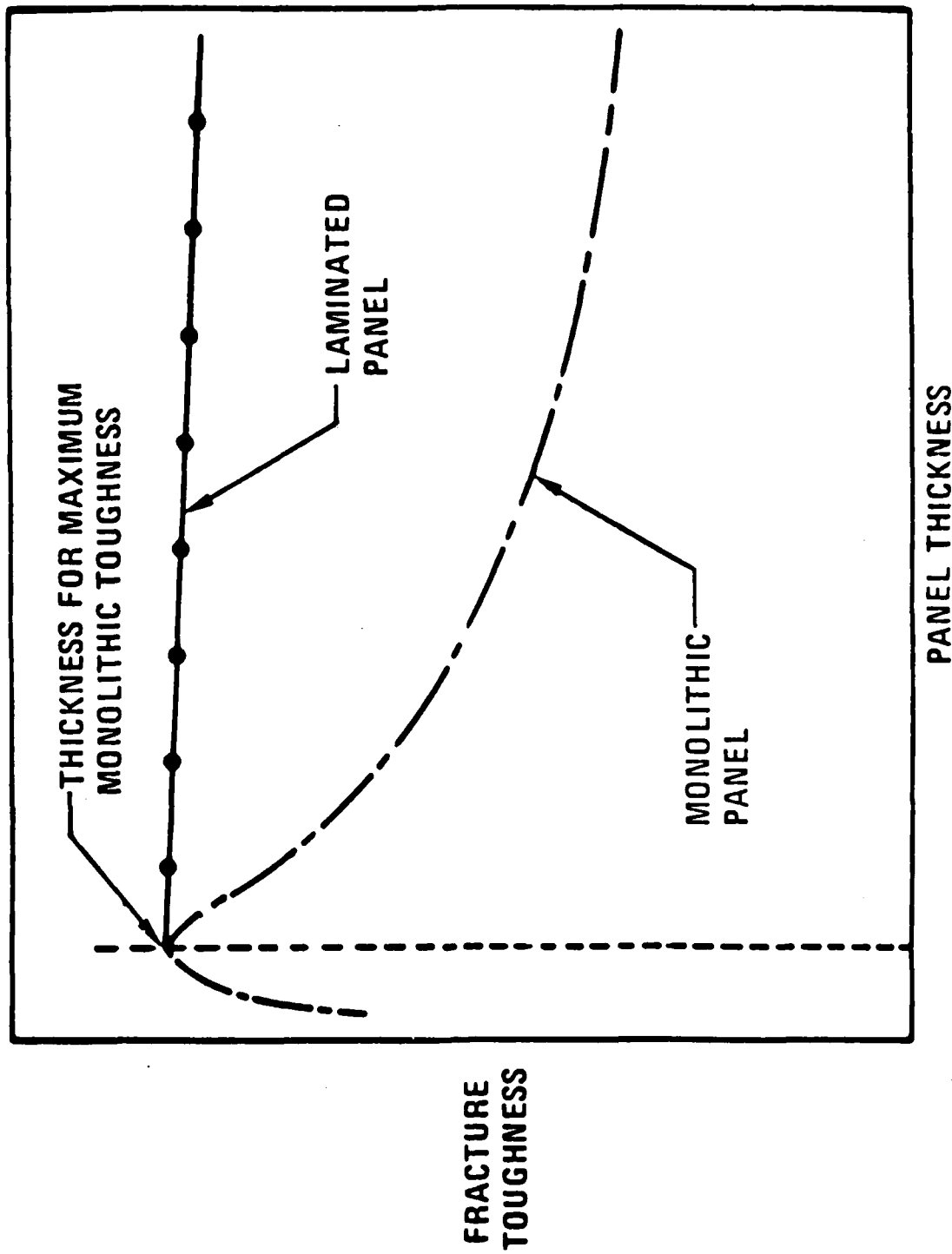


FIGURE 4. FRACTURE TOUGHNESS VERSUS THICKNESS FOR MONOLITHIC AND LAMINATED MATERIALS (SCHEMATIC).

as mechanical and chemical stability, and improved wear resistance and corrosion resistance through the proper choice of layer and interleaf alloys, the geometry of the laminate lay-up, and the processing and heat treating variables.

In previous years of the Metal Laminates for Structures Program the metal-metal laminate concept has been validated and various fabrication techniques explored. During the first year of the program, seven laminate configurations were fabricated using three processing techniques; diffusion bonding roll bonding, and explosion bonding. The materials systems investigated were 7475 Al/1100 Al (the alloy designated to the left of the slash mark is the primary or layer alloy; the alloy to the right, the interleaf), 7075 Al/7072 Al, and Ti-6Al-4V/6061 Al. The mechanical properties - strength, fracture toughness, and fatigue strength - of each laminate system were evaluated and compared with similarly heat treated monolithic alloys.⁴ During the second year of the program, diffusion bonded 7475 Al/1100 Al, 7475 Al/1100 Al, 7075 Al/7072 Al, Ti-6Al-4V/CP-Ti, ultrahigh carbon steel/interstitial free iron; adhesively bonded 7475 Al and 7075 Al; and roll bonded 7475 Al/1100 Al were evaluated similarly.³³ In the third year the further development of roll bonding procedures and heat treating parameters was effected for several steel and titanium alloy systems. Specifically studied were 300M/AISI 1020, 300M/SAE 1075, and 300M/AISI E52100, Ti-6Al-4V/CP Ti, Ti-10V-2Fe-3Al/Ti-15V-3Cr-3Al-3Sn, Ti-8Al-2V-6Cr-4Zr-4Mo/CP Ti, and Ti-8Al-8V-6Cr-4Zr-4Mo/Ti-15V-3Cr-3Al-3Sn. In addition to the tensile and fracture toughness of these alloy laminate systems, the axial fatigue properties of representative alloys were evaluated. Finally, the use of several interleaf alloys in the 300M steel system allowed the conjoint nature of interleaf properties, interlaminar bond properties, and layer properties to be evaluated, and the inverse relationship between layer thickness and fracture toughness was substantiated.³⁵ Some results for several laminate systems investigated in the Program are listed in Table 1.

Although many items may be fabricated directly from plate, numerous other structural components benefit from the material utilization efficiency and forming economy occasioned by forging. In addition, the mechanical properties of many components may be improved by the flow or fibering that obtains during forging. Nevertheless, the forgeability of laminates and the effects of forging on roll-bonded metal-metal laminates had not been determined. Furthermore, laminates present several unique problems in forging since the improved

TABLE 1. FRACTURE TOUGHNESS IMPROVEMENT FOR SEVERAL METAL-METAL LAMINATES

PRIMARY ALLOY	INTERLEAF	TENSILE STRENGTH ksi(MPa)	MONOLITHIC TOUGHNESS ksi - in. ^{1/2} (MPa-m ^{1/2})	LAMINATE TOUGHNESS, ksi - in. ^{1/2} (MPa-m ^{1/2})	TOUGHNESS IMPROVEMENT (REFERENCE)
300M STEEL, 0.16 in. (4.06mm) LAYER THICKNESS	1020 STEEL	250 (1724)	61(67)	135(148)	121% (35)
300M STEEL 0.061 in. (1.55 mm) LAYER THICKNESS	1020 STEEL	236 (1627)	61(67)	209(230)	242% (36)
7075 ALUMINIUM	7072 Al	76 (524.0)	40(44)	60 (66)	50% (33)
7475 ALUMINIUM	1100 Al	77 (530.9)	60(66)	90 (99)	50% (33)
TITANIUM-10V-2Fe-3Al	Ti-15V-3Cr-3Al-3Sn	187 (1289)	38(42)	88 (97)	114% (35)
TITANIUM-6Al-4V	6061Al	140 (965.3)	57(63)	124(136)	117% (4)

fracture toughness of laminates is dependent on delamination and the fiber of laminates is intrinsic and cannot be easily reoriented. The present study, therefore, was undertaken to determine the forgeability of a roll-bonded metal-metal laminate system in several orientations and the effects of forging on the structure and properties, especially the fracture toughness, of metal laminates. In addition, the stress corrosion cracking properties of roll-bonded material were to be determined, since it had been suggested earlier that these laminate material systems would offer significant benefits in stress corrosion cracking resistance in the crack divider orientation. Specifically, the following tasks were performed for the study:

- o Metal-metal laminate plate stock of 300M alloy steel interleaved with 1010 mild steel was fabricated by hot roll bonding.
- o Specimens taken from the plate stock and monolithic controls were forged in an open die. The laminate was forged in both the longitudinal and transverse orientations.
- o The physical and mechanical properties of the forged laminates and controls were determined when possible.
- o Several laminate specimens were forged in a more complex closed die and the mechanical properties of these forgings determined.
- o The high cycle fatigue strength of roll-bonded laminate plate was compared with monolithic control plate.
- o The stress corrosion cracking rate of roll-bonded laminate plate and the critical stress intensity factor for stress corrosion cracking were determined and compared with a monolithic control.

2.0 EXPERIMENTAL PROCEDURE

2.1 MATERIAL SELECTION

During the execution of a prior study³⁵ the significant toughness improvements obtainable in an ultrahigh strength steel/mild steel laminate system fabricated by roll bonding were demonstrated. The most successful steel system studied consisted of layers of 300M alloy steel (MIL-S-8844C,³⁸ Class 3) interleaved with AISI-SAE 1020 mild steel. Since 300M is a common aerospace forging alloy that is used at high strength levels in critical applications, such as aircraft landing gear and arresting gear, a laminate system based on 300M was determined to be a desirable choice for the study of laminate forgeability. Furthermore, a significant data base on roll-bonded 300M systems had already been accumulated and could be used for comparison. The specific material combination chosen consisted of eighteen layers of 300M interleaved with seventeen layers of AISI-SAE 1010 mild steel.

2.2 LAMINATE PREPARATION

A 3/4 inch (19 mm) plate of steel alloy 300M (MIL-S-8844C, Class 3) weighing approximately 390 pounds (177 kg) was obtained from Friend Metals, Anaheim, California. The mill chemical analysis of this plate is listed in Table 2 in which it is also compared with the specified chemical analysis. Since a one-fourth inch (1/4 in., 6.35mm) starting thickness was required for the laminate lay-up prior to roll bonding, plates of 6 x 8 inches (152 x 203mm) dimensions were flame cut from the parent plate and rolled to the one-fourth inch (6.35 mm) starting thickness required at the Jones and Laughlin Steel Corporation Graham Research Laboratories, Pittsburgh, Pennsylvania. A start temperature of 2150°F (1177°C) was used for the rolling, and the reduction of 67 percent was accomplished without reheating. Following rolling, the 300M plates were cut into approximately 17 inch (432 mm) lengths, grit blasted, degreased, and laid up with interleaves of commercially obtained AISI-SAE 1010 mild steel (Table 3) sheets approximately 0.030 inch (0.76 mm) thick to form an eighteen layer, seventeen interleaf metal-metal laminate lay-up, approximately 5.35 inches (136 mm) in height. Finally, the laminate

TABLE 2. CHEMICAL COMPOSITION OF ALLOY 300M

ELEMENT	CONTENT, WEIGHT PERCENT	
	SPECIFIED*40	MILL ANALYSIS
C	0.40-0.45	0.420
Mn	0.65-0.90	0.74
Si	1.45-1.80	1.73
Ni	1.65-2.00	1.83
Cr	0.65-0.90(0.70-0.95)	0.86
Mo	0.30-0.45(0.35-0.45)	0.41
V	0.05 MIN	0.09
P	0.025 MAX (0.010 MAX)	0.006
S	0.025 MAX (0.010 MAX)	0.004
Cu	---	0.16
Fe	Balance	---

*MIL-S-8844C requirements which differ from commercial 300M are listed in parentheses.

TABLE 3. CHEMICAL COMPOSITION OF
AISI-SAE 1010 AND 4145 STEELS⁴¹

ELEMENT	CONTENT, WEIGHT PERCENT	
	1010	4145
C	0.08-0.13	0.43-0.48
Mn	0.30-0.60	0.75-1.00
P	0.040 MAX	0.035 MAX
S	0.050 MAX	0.040 MAX
Si	0.60 MAX	0.15-0.30
Cr	---	0.80-1.10
Mo	---	0.15-0.25
Cu	0.060 MAX	---
Fe	Balance	Balance

lay-up was boxed in a 1010 mild steel box and the box welded closed. The purpose of the box was the stabilization of the laminate during the initial rolling prior to complete bonding and the protection of the surfaces during heating and processing. The boxed laminate lay-up was roll bonded by hot rolling using a start temperature of 2150°F (1177°C) and an overall reduction in area of 44 percent. The rolling was accomplished without reheating using roll reductions of approximately 10 percent per pass and six passes on a 1000 kip (4.5 MN) reversing mill at the U.S. Steel Corporation Research Laboratories, Monroeville, Pennsylvania. The final thickness of the roll-bonded laminate was three inches (76 mm). Bonding was complete in the center of the laminate billet, although there was a central delamination at each end. The delamination extended approximately three inches (76 mm) into the billet at one end and one inch (25 mm) at the other. The material above and below the plane of delamination was bonded, however. The as-roll-bonded laminate billet following the removal of the delaminated end is shown in Figure 5. The cut end has been macroetched with dilute nitric acid to reveal the layered structure.

2.3 FORGEABILITY TESTING

The forgeability test chosen for the laminate and control material was the upset test.³⁹ This procedure consists of upsetting identical cylinders of material to varying thicknesses or cylinders with differing height to diameter ratios to the same final thickness. Since it was desired to use the full thickness of the laminate billet and to decrease the relative effects of friction through the constancy of initial contact area, the latter method of upset testing, viz., the varying height to diameter ratio, h_0/d_0 , method was chosen for the longitudinal and control forgings. The choice of this method also facilitated the mechanics of testing in that a single stop block could be used for all the tests, this method being the only viable one for controlling thickness in the large hydraulic open die press used. The limited laminate billet thickness, however, necessitated the upsetting of flat plates of material to varying heights for transverse upset testing, but the small relative change in surface area during forging did not pose any problems vis à vis friction. For the longitudinal forgeability testing the laminate billet was cut into three inch (76 mm), four inch (102 mm), and five inch (127 mm) blanks and these were turned to form cylinders 2 7/8 inches (73.03 mm) in diameter

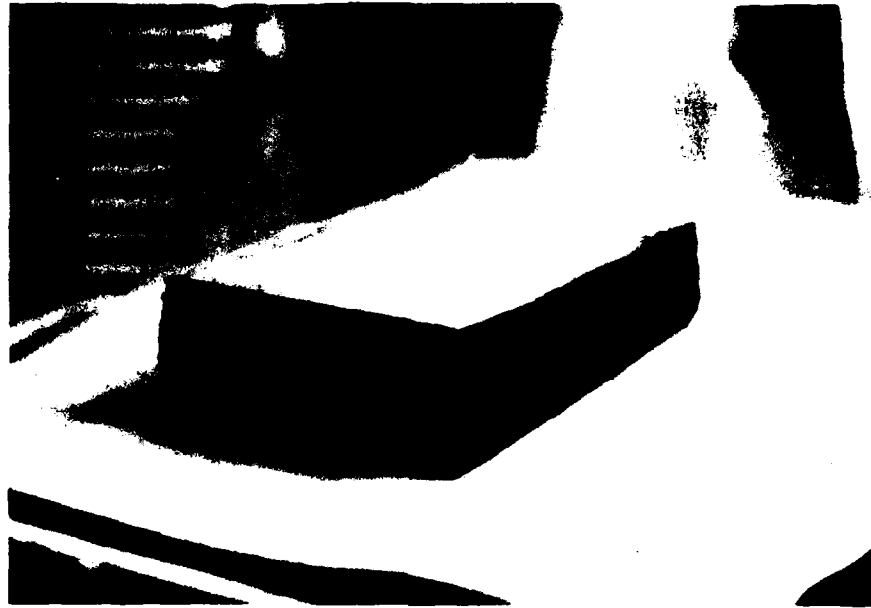


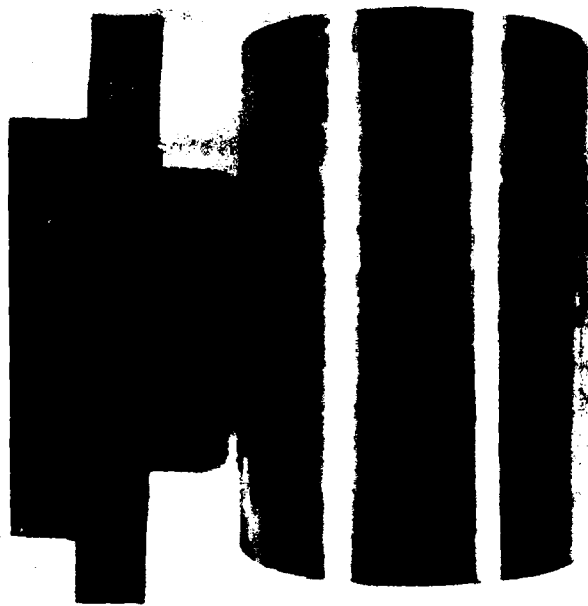
FIGURE 5. AS ROLL-BONDED 300M/1010 LAMINATE BILLET. THE CUT END HAS BEEN MACROETCHED WITH NITRIC ACID. THE BILLET DIMENSIONS AS SHOWN ARE $2 \frac{7}{8} \times 6 \frac{3}{8} \times 13 \frac{5}{8}$ INCHES. (73 x 162 x 346 mm)

and of the following nominal lengths: 2.5 in. (64 mm), 3 in. (76 mm), 4 in. (102 mm), 4 in. (102 mm), 5 in. (127 mm), and 5 in. (127 mm). In addition, comparison cylinders were turned from a four inch (102 mm) square rolled billet of AISI-SAE 4145 low alloy steel such that the axis of the cylinder corresponded to the rolling direction of the parent billet. The specified composition ranges for 4145 are listed in Table 3. The 4145 cylinders were also 2 7/8 inches (73 mm) in diameter and, respectively, 3 in. (76 mm), 4 in. (102 mm), and 5 in. (127 mm) in length. In all cases particular attention was paid toward the parallelism of the machined cylinder ends. One of the as-turned laminate cylinders is shown in Figure 6. In addition to the cylinders, four transverse forging specimens were prepared of the following dimensions in inches (mm): 6.250 x 3.750 x 1.375 (158.75 x 95.25 x 34.93), 6.688 x 4.125 x 1.875 (169.88 x 104.78 x 47.63), 4.250 x 2.625 x 1.332 (107.95 x 66.68 x 33.83), and 4.250 x 2.625 x 1.616 (107.95 x 66.68 x 41.05). In this and following discussions longitudinal forging refers to processing in which the direction of ram travel lies in the laminar plane of a laminate specimen or is coincident with the rolling direction of the monolithic billet; the forging plane is normal to the laminar plane or monolithic fiber. Transverse refers to the inverse orientation of the laminate, i.e., the ram direction is perpendicular and the forging plane is parallel to the laminar plane.

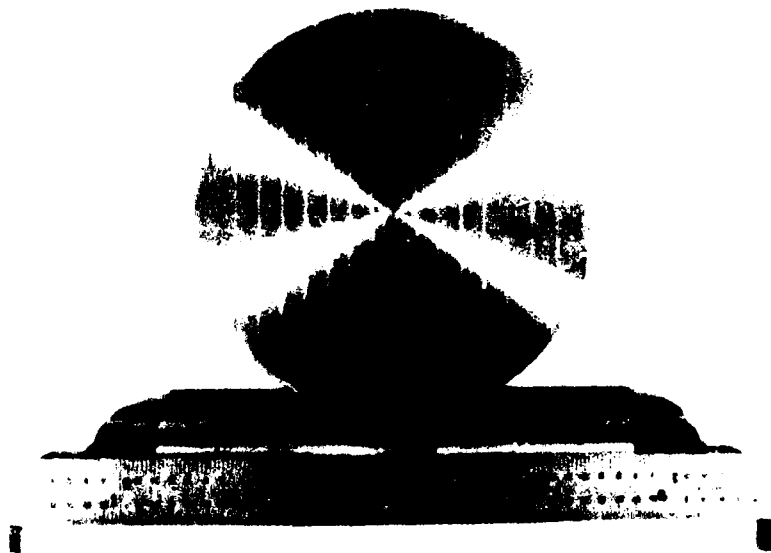
The upset forging was performed on a 3300 ton (29.4 MN) hydraulic press at the Beaumont Well Works Company, Houston, Texas, using flat, parallel open dies and a start temperature of 2200°F (1204°C). Lubrication was provided by woven glass cloth placed between the hot specimen and the dies. Forging speed was in the range of 0.25 - 1.0 ft/s (0.08-0.30 m/s). Final height of the longitudinal cylinders was controlled to between 2 and 2.5 inches (51 and 64 mm) nominally and to between 0.5 and 1 inch (13 and 25 mm) for the transverse specimens.

2.4 COMPLEX FLOW EVALUATION

Although the open die testing was designed to provide the requisite information on forgeability in simple flow geometries, it did not simulate the more complex material flow often required in the forming of a complex structural item. Therefore, a closed die forging of more complex shape was chosen to supplement the open die forgeability testing. In order to minimize the costs



(a)



(b)

FIGURE 6. LAMINATE LONGITUDINAL FORGEABILITY CYLINDER.

associated with the closed die forging, it was necessary to use an existing production die and, of course, standard production equipment. The die chosen was that for a gear blank. The part produced from this die resembled a wheel and hub. The forging print for this part with flash removed is reproduced in Figure 7. As may be noted in the figure the item consisted of a central hub surrounded by a circular web and a circumferential flange.

The roll-bonded stock material for the closed die forging was fabricated identically with that used in the open die forgeability tests, that is, a second billet was laid up and roll bonded as described in Section 2.2. This billet was sectioned and the blanks turned to produce six cylindrical preforms approximately 3 1/4 inches (82.6 mm) in diameter and 2 7/8 inches (73 mm) in height. The presence of a large lamination in the billet, however, prevented the fabrication of more than one preform of this height, the other five being approximately 1 7/8 inches (48 mm) in height. Although these later five preforms did not throw flash, they did very nearly fill the die and did form the outer flange. The process schedule for the closed die forging is summarized schematically in Figure 8. The forging itself was performed on a board hammer at the Pittsburgh Forgings Company Coraopolis, Pennsylvania, plant. The preforms were heated in a gas fired slot furnace to approximately 2400°F (1316°F) and then forged, the full height preform requiring 27 blows and the remaining five preforms eight or nine blows each. Following forging each of the material specimens were annealed and either sectioned and examined or machined for mechanical testing.

2.5 PHYSICAL EVALUATION

Following forging each forgeability specimen was visually examined then subcritically annealed at 1275°F (691°C) for two hours, the A_{c1} for 300M being approximately 1400°F (760°C), in order to facilitate the machining of mechanical test specimens from the forgings. Of course, prior to machining the forgings were photographically documented and examined for physical integrity. Samples were also taken from the forgings for metallographic examination, particular attention being paid to the layer-interleaf interface and its integrity.

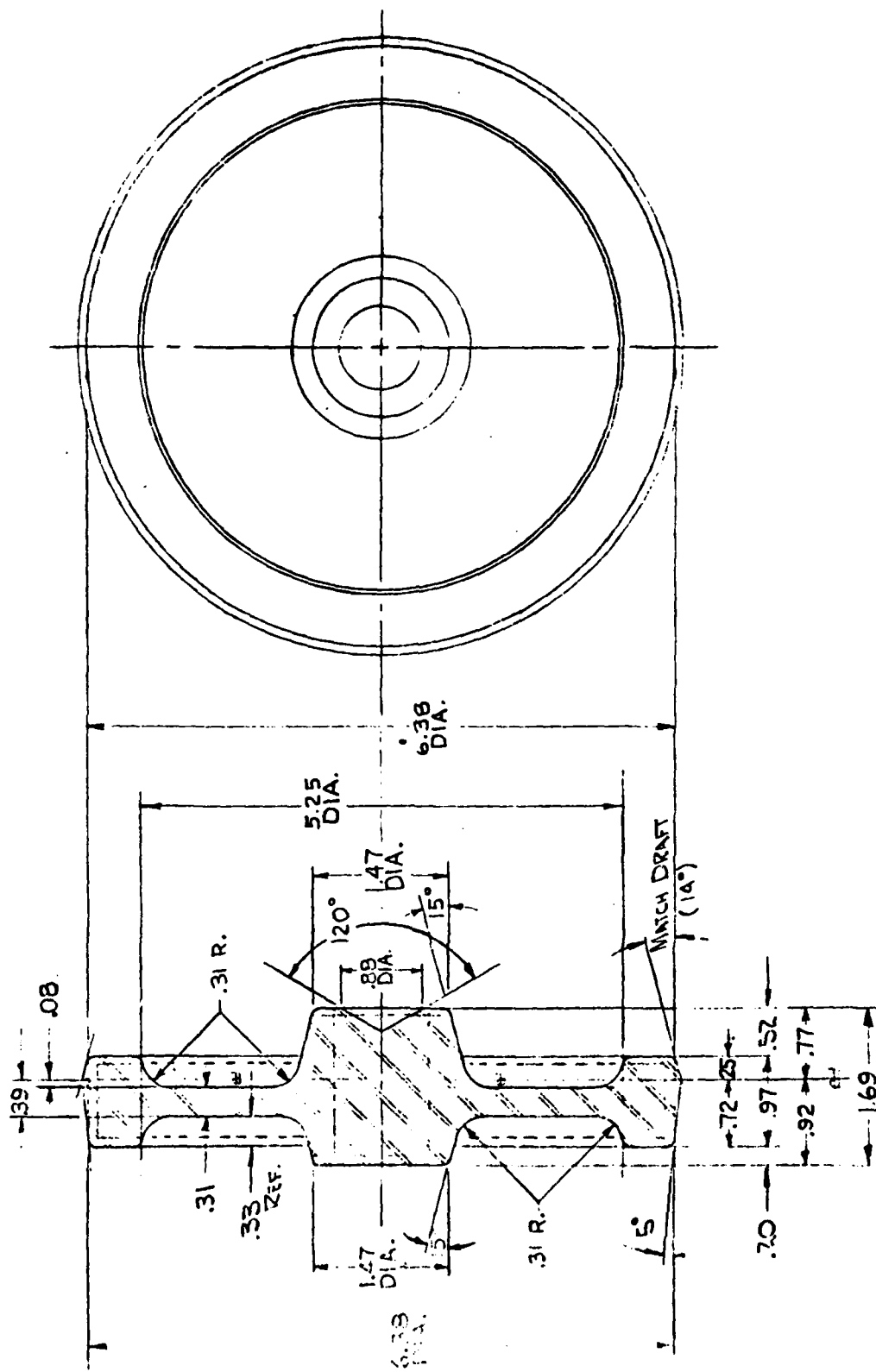


FIGURE 7. FORGING PRINT OF THE CLOSED DIE FORGING, A REDUCTION GEAR BLANK.

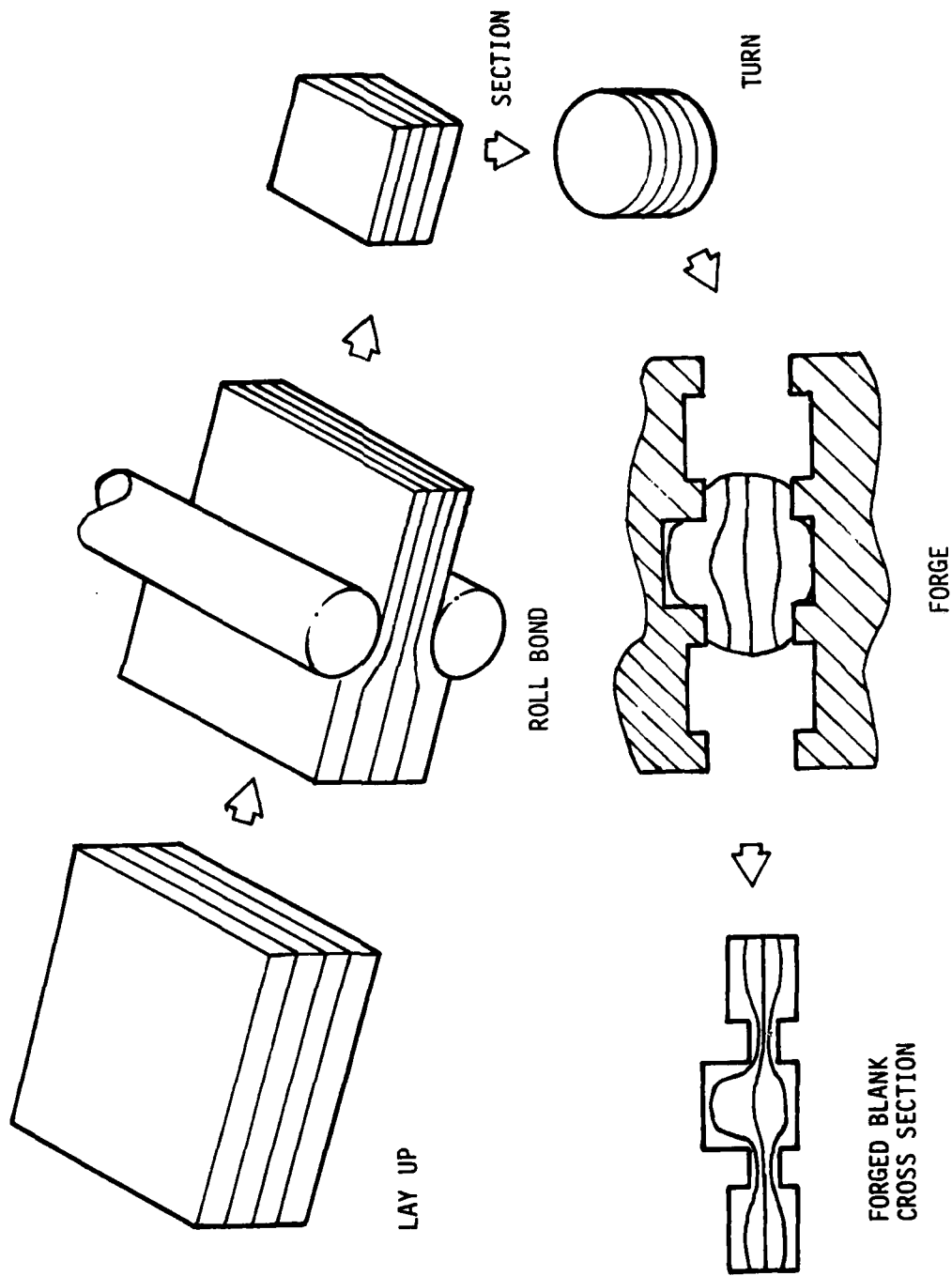


FIGURE 8. SCHEMATIC PROCESS FLOW FOR LAMINATED CLOSED DIE FORGEABILITY TESTING.

2.6 HEAT TREATMENT

All the specimens were heat treated so as to produce strength levels that were near the practical maximum for 300M steel, since the value of metal laminates has been shown to be primarily in the retention of fracture toughness at ultrahigh strength levels. The specific heat treatment schedule used was the following: normalize at 1700°F (927°C) for 1/2 hour (1.8 ks), air cool to approximately 400 - 500°F (204-260°C), austenitize at 1600°F (871°C) for 1/2 hour (1.8 ks), oil quench, temper at 575°F (302°C) for two hours (7.2 ks), air cool, and repeat temper. This heat treatment produces an ultimate tensile strength for 300M greater than 250 ksi (1724 MPa).

2.7 MECHANICAL TESTING

Following heat treatment the mechanical properties of those forgings from which sufficient mechanical test specimens could be machined were evaluated through tensile and fracture toughness testing. In addition, the important physical properties of the specimens, such as the thicknesses of the individual layers and interleaves and the average layer thickness were determined.

2.7.1 Tensile Properties

Tensile specimens were cut from the as-rolled and the forged material where possible in accordance with American Society for Testing and Materials (ASTM) Standard E 8 for plate.⁴² Tensile testing was accomplished in accordance with ASTM E 8, and the following tensile properties were determined: the 0.2 percent offset yield strength, the ultimate tensile strength, the tensile elongation or elongation to fracture, the uniform elongation, the true strain at the onset of necking (maximum load) or the true uniform elongation, and the true stress at necking (maximum load).

2.7.2 Fracture Properties

The fracture toughness of laminates and monolithic materials was determined from standard, ASTM E 399,⁴³ compact tension specimens. These specimens were machined from the annealed material, heat treated, and then pre-cracked in accordance with ASTM E 399. Specimens were machined from the plate

and forgings in as many orientations as were compatible with the processed material. All specimens were of crack divider type, since this is the toughness controlling orientation expected in most laminate structural items. Figure 9 illustrates schematically the compact tension specimens orientation with respect to the flow of the parent material, either plate or forging. Fracture toughness parameters were calculated from measurements of the loads and the corresponding crack opening displacements (COD) experienced by the compact specimens during testing. Three stress intensity factor toughness parameters were calculated as follows:

- o K_Q - The conditional fracture toughness calculated using the 95 percent secant load (ASTM E 399) and the calculated (COD) crack length corresponding to that load.
- o K_A - the apparent fracture toughness calculated using the maximum load and the same crack length as K_Q .
- o K_C - the critical fracture toughness calculated using the maximum load and the effective calculated crack length (from COD) corresponding to maximum load.

In all cases fracture toughness, K_X , is defined as follows:

$$K_X = \frac{P_f}{BW^{1/2}} f(a/W)$$

- P_f = load at failure or crack extension,
- B = specimen thickness,
- W = specimen width, and
- a = crack length at crack extension or failure.

In addition to the above toughness parameters, the specimen strength ratio,⁴³

$$R_{SC} = \frac{2P_{MAX}(2W+a)}{B(W-a)^2\sigma_y}$$

where

- P_{MAX} = maximum load sustained
- W = specimen width,
- a = crack length,
- B = specimen thickness, and
- σ_y = the 0.2 percent offset yield strength

was calculated.

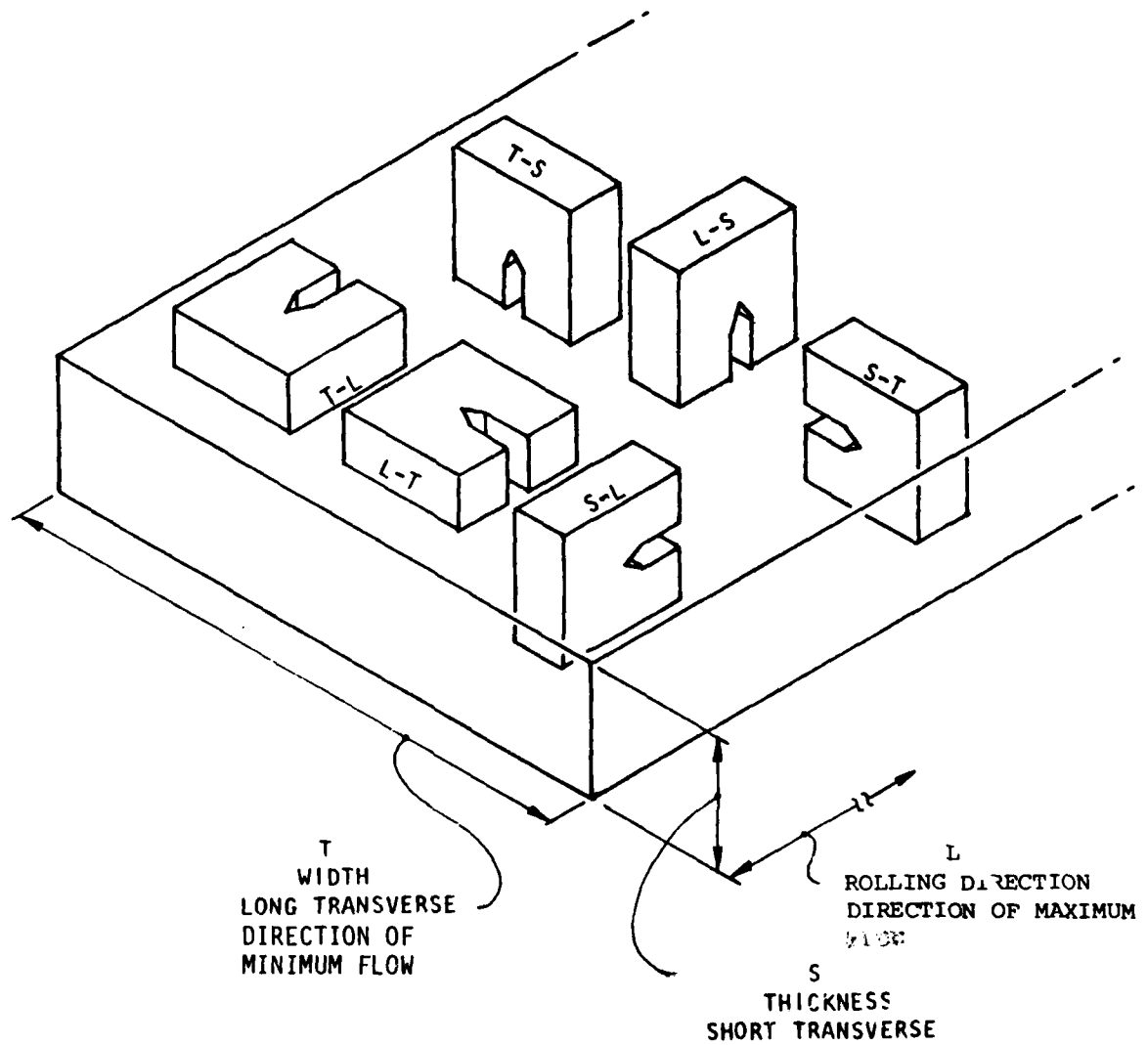


FIGURE 9. SCHEMATIC ILLUSTRATION OF CRACK PLANE ORIENTATION WITH RESPECT TO THE ORIENTATION OF THE PARENT MATERIAL. AFTER ASTM E 399, REFERENCE 43.

2.7.3 Fatigue Strength

The fatigue strength of roll-bonded laminates was compared with monolithic 300M through the generation of stress versus cycles-to-failure data. All fatigue tests used cylindrical specimens machined such that the longitudinal axis of the specimen corresponded to the rolling direction of the laminate billet or monolithic plate. The fatigue tests were conducted in axial tension with a load ratio, $R = \text{minimum load}/\text{maximum load}$, of 0.1 at a frequency of 30 Hz in air.

2.8 STRESS-CORROSION CRACKING EVALUATION

The stress corrosion cracking properties; crack propagation rate, da/dt , and the critical stress intensity factor for stress corrosion cracking, $K_{I_{SCC}}$; were determined for roll-bonded 300M/1010 material in the crack divider orientation and compared with monolithic 300M. These tests were conducted using bolt-loaded (self-loaded) compact tension specimens. Following heat treatment these specimens were cleaned, precracked, degreased, loaded, and placed in the 3.5 percent sodium chloride (NaCl) aqueous solution. Periodic optical measurements were made to determine the crack growth as a function of time. The $K_{I_{SCC}}$ of each specimen was considered to be that stress intensity factor at which no growth had been discernible for at least one hundred hours (360 ks).

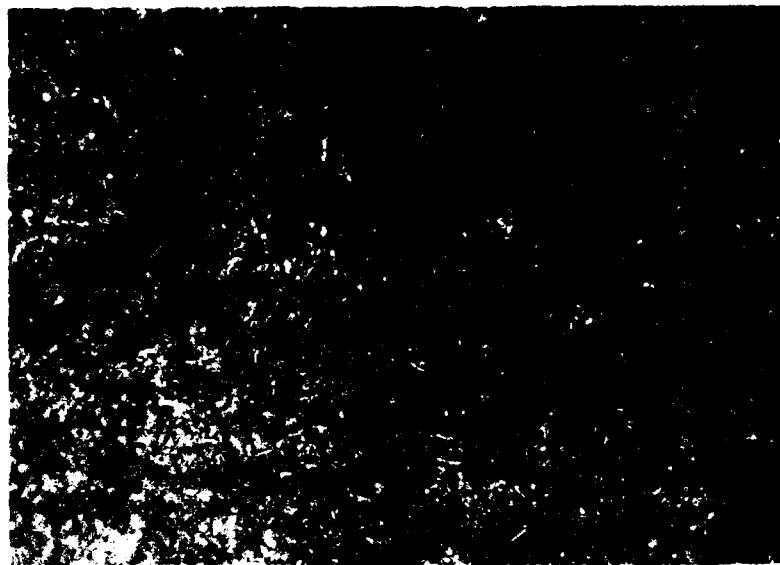
3.0 RESULTS AND DISCUSSION

3.1 LAMINATE PREPARATION

As noted previously (Section 2.2) the ends of the roll-bonded billet failed to bond at the center lamina. This problem has been encountered before and appears to be primarily a result of tensile stresses generated because of insufficient penetration of the plastic zone during rolling. This problem is analogous to the alligating sometimes encountered in the rolling of plate.⁴⁴ Of course, prior to the obtainment of inter-layer bonding, the short transverse strength of the laminate is essentially zero and it cannot resist the splitting. An additional problem also obtains in the roll bonding of laminate lay-ups that can lead to or exacerbate the alligating phenomenon. This could be called the flat die or seesaw effect and results from the tendency of long plates compressed at one end to spread apart at the other, that is to act as independent beams. This response is manifest in rolling laminates primarily when the laminate thickness is small in comparison to the roll diameter. In order to prevent its occurrence the lay-up must be stabilized against tensile failure effectively in the short transverse direction. In roll bonding of laminates it is desirable, therefore, in addition to plate stabilization and atmospheric protection, to provide short transverse tensile hot strength especially at the front and rear end of the lay up. This may be done by welding the laminate and providing sufficient weld metal at the ends to carry the load, e.g., provide a single-U or -V groove weld of sufficient depth between layers; strapping the ends of the lay-up with a doubler plate either welded or clamped on; or boxing the laminate and strengthening the front and rear ends of the box.

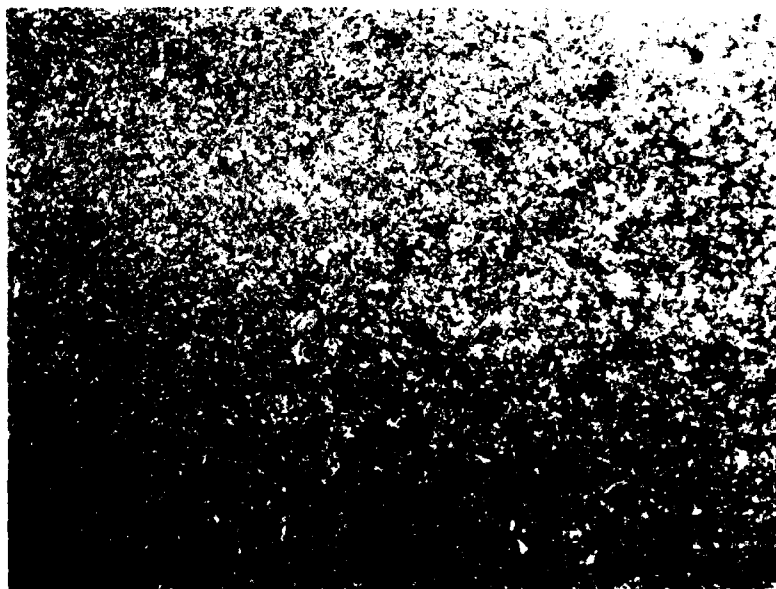
3.1.1 Laminate Micrography

The microstructure of the base 300M steel is shown in Figures 10 and 11 in the quenched and tempered condition. The steel as shown is completely comprised of a very fine tempered martensite as expected for a through hardening low alloy steel of this type. In addition, it may be noted that the microstructure of steel is very clean, that is there are few non-metallic inclusions visible. This is also typical of a vacuum arc remelted steel of aircraft quality.



100 μm

FIGURE 10. 300M STEEL, QUENCHED AND TEMPERED, LONGITUDINAL SECTION. MAGNIFICATION: 200X. 2% NITAL ETCHANT.



50 μm

FIGURE 11. DETAIL OF FIGURE 10. MAGNIFICATION: 500X. 2% NITAL ETCHANT.

Following roll bonding the laminate plate was subcritically annealed at 1275°F (691°C) for two hours (7.2 ks) in order to produce a fully spheroidized structure that could be easily machined. The microstructure of the as-rolled and annealed laminate is shown in Figures 12, 13, and 14. Since the 300M transforms even on air cooling to martensite and bainite,⁴⁵ it may be fully spheroidized by a subcritical anneal, i.e., held at a high temperature below A_{c1} . The fine structure of the 300M evidenced in the micrographs is a very fine spheroidite plus some coarse tempered bainite. The ferritic-pearlitic structure of the 1010 obtained upon cooling is essentially unchanged by the anneal. An interesting microstructural effect may be noted near the bond line, however, in that there appears to be a spheroidized layer just within the 1010 interleaf and a light etching layer adjacent to the bond line, predominately in the 300M. It is felt that this "spheroidite free zone" results from the diffusion of alloying elements, especially carbon, into the 1010 during rolling thus allowing the layer within the 1010 to transform on cooling such that it will later spheroidize. The light etching layer, then, would appear to be a zone depleted by the ripening of the spheroidal cementite within the parent 1010 during spheroidization. The kinetics and directionality of both the transdiffusion and the depletion may be aided by the high silicon content of the 300M. This is analogous to the under surface decarburization that is sometimes noted in carburized 300M.⁴⁶ Subsequent micrographs of quenched and tempered material illustrate the hardenability of the interdiffusion layer in the parent 1010 interleaf. In the quenched and tempered case, however, the depleted layer disappears, since the material transport during tempering is not as long range as that during spheroidization.

Figures 13 and 14 also illustrate the as roll-bonded condition of the layer-interleaf bond line. It may be noted, particularly in Figure 14, that the metallurgical bond is quite extensive with some apparent recrystallization across the bond line. The bond line is also quite clean, although there is some porosity distributed along the interfacial bond line.

3.2 FORGEABILITY TESTING

The numerical results of the hot forgeability testing are contained in Table 4. It may be noted that engineering strains between approximately -23 percent and -55 percent were investigated for the longitudinal cylinders, and,

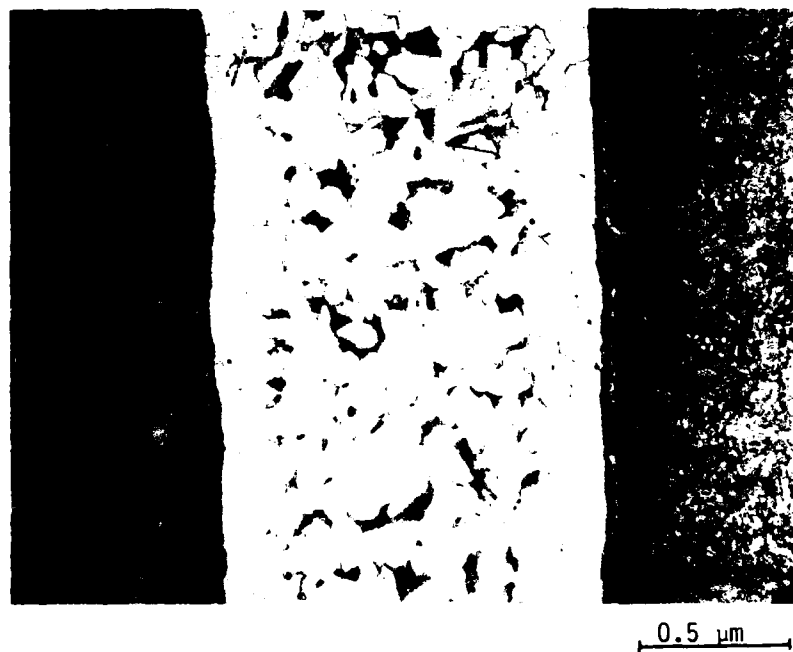


FIGURE 12. 300M/1010 AS ROLL-BONDED LAMINATE, ANNEALED, LONGITUDINAL SECTION. THE CENTER LAMINA IS THE 1010 INTERLEAF. MAGNIFICATION: 44X. 2% NITAL ETCHANT.



FIGURE 13. 300M/1010 AS ROLL-BONDED LAMINATE, ANNEALED, TRANSVERSE SECTION. THE 1010 INTERLEAF IS AT THE LEFT. MAGNIFICATION: 200X. 2% NITAL ETCHANT.



FIGURE 14. 300M/1010 AS ROLL-BONDED LAMINATE, ANNEALED LONGITUDINAL SECTION. THE 1010 INTERLEAF IS AT THE LEFT. MAGNIFICATION: 500X. 2% NITAL ETCHANT.

TABLE 4: HOT UPSET FORGEABILITY RESULTS

MATERIAL, ORIENTATION, SPECIMEN	INITIAL LENGTH, in. (mm)	FINAL LENGTH, in. (mm)	STRAIN, %	TRUE STRAIN, %	INITIAL DIAMETER, in. (mm)	FINAL MAJOR AXIS, in. (mm)	FINAL MINOR AXIS, in. (mm)	UPSET RATIO, 1/d ₀
300M/1010, L, 4B	2.461 (62.51)	1.805 (45.85)	-26.7	-31.0	2.875 (73.03)	3.530 (89.66)	3.520 (89.41)	0.228
300M/1010, L, 4A	2.923 (74.24)	2.246 (57.05)	-23.2	-26.4	2.875 (73.03)	3.480 (88.39)	3.480 (88.39)	0.236
300M/1010, L, 5A	4.002 (101.65)	2.295 (58.29)	-42.7	-55.6	2.875 (73.03)	4.610 (117.09)	3.470 (88.14)	0.594
300M/1010, L, 5B	3.995 (101.47)	1.880 (47.75)	-52.9	-75.4	2.875 (73.03)	5.100 (129.54)	4.470 (113.54)	0.736
300M/1010, L, 6A	5.000 (127.00)	2.335 (59.31)	-53.3	-76.1	2.875 (73.03)	5.475 (139.07)	4.015 (101.98)	0.927
300M/1010, L, 6B	5.000 (127.00)	2.236 (56.79)	-55.3	-80.5	2.875 (73.03)	5.535 (140.59)	4.831 (122.71)	0.961
4145, L, 7A	3.050 (77.47)	1.986 (50.44)	-34.9	-42.9	2.875 (73.03)	3.700 (93.98)	3.700 (93.98)	0.370
4145, L, 8A	4.010 (101.85)	2.535 (64.39)	-36.8	-45.9	2.875 (73.03)	3.836 (97.43)	3.836 (97.43)	0.513
4145, L, 9A	5.005 (127.13)	2.275 (57.79)	-54.6	-78.9	2.875 (73.03)	4.485 (113.92)	4.485 (113.92)	0.950
300M/1010, T, 10	1.375 (34.93)	0.849 (21.57)	-38.3	-48.2	7.289 (185.14)	-----	-----	0.072
300M/1010, T, 11	1.875 (47.63)	0.830 (21.08)	-55.7	-81.5	7.858 (199.59)	-----	-----	0.133
300M/1010, T, 12	1.332 (33.83)	0.560 (14.22)	-58.0	-86.7	4.995 (126.87)	-----	---	0.155
300M/1010, T, 13	1.616 (41.05)	0.588 (14.94)	-63.6	-101.1	4.995 (126.87)	-----	---	0.206

between approximately -38 percent and -64 percent, for the transverse forgings. In all cases some delamination or edge cracking occurred in the longitudinal forging of the laminate cylinders, whereas no edge cracking or center cracking occurred in the 4145 monolithic control cylinders. The transverse laminates also were forged successfully. The upset cylinders exhibited four post-forged forms as shown in Figures 15 through 19. Figure 15 illustrates the stable barrelling of all the 4145 cylinders. No edge cracking or center cracking was discernable. In Figure 16 is illustrated the least severe upset test of a laminate cylinder in which barrelling has been accompanied by some edge cracking. Nevertheless, many of the laminae remained bonded as shown in Figure 17. Upon more severe deformation the laminates generally buckled in one of two modes as shown in Figures 18 and 19. The first mode shown in Figure 18 was complete buckling of all laminae leaving a central hole through the forged laminate. A second mode shown in Figure 9 was observed in several specimens in which several of the center layers were stabilized by the buckled outer layers and were upset almost stably, although some local buckling in each of the specimens within these center layers prevented the retention of a good bond after forging. No cracking or buckling were encountered in the transversely forged laminates, although some uneven flow due to friction obtained as shown in Figures 20-22. The phenomena of barrelling and buckling and the effect of friction will be discussed subsequently in greater detail; however, several operational conclusions concerning the forgeability of these metal-metal laminates are justified on the basis of the hot forgeability testing. These conclusions are (1) the forgeability in the longitudinal direction is limited to approximately -27 percent strain, (2) for specimens forged to strains of approximately -53 percent and more the mode of failure was hot buckling rather than edge cracking, and (3) the laminates may be forged successfully to strains of at least -63 percent in the transverse direction.

The hot upset testing and results discussed above represent the most severe forging conditions expected for a metal laminate in the longitudinal orientation. The severity of upsetting is related primarily to the magnitude of the frictional traction that acts on the specimen in contact with the die. In all the upset tests a chemical reaction between the vitreous lubricant cloth used and the forgeability specimen led to essentially a condition of sticking friction. This means that there was no relative movement between the



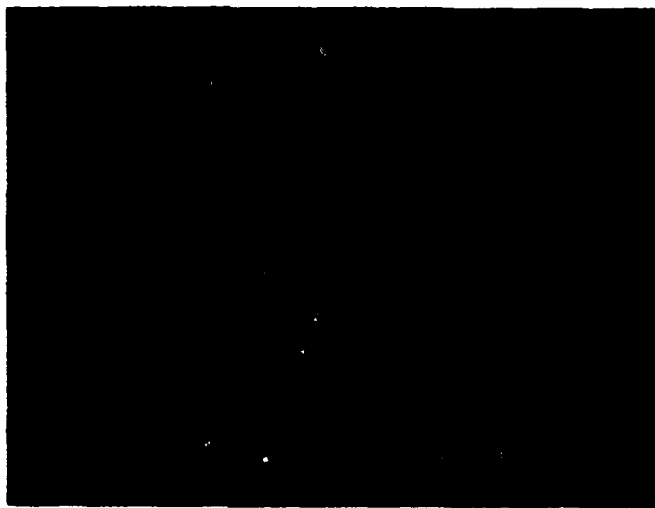
10mm

FIGURE 15. UPSET MONOLITHIC SPECIMEN 9A EXHIBITING STABLE BARRELLING AND A LACK OF EDGE CRACKING.



10mm

FIGURE 16. UPSET SPECIMEN 4A EXHIBITING EDGE CRACKING.



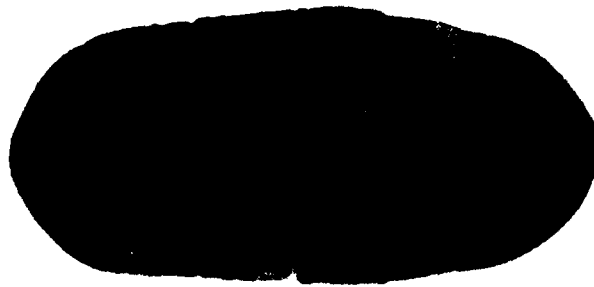
10 mm

FIGURE 17. UPSET SPECIMEN 4A (FIGURE 16) DETAIL.
MAGNIFICATION: 2X.



10mm

FIGURE 18. UPSET SPECIMEN 6A EXHIBITING HOT BUCKLING.



10mm

FIGURE 19. UPSET SPECIMEN 6B EXHIBITING BOTH HOT BUCKLING AND STABLE UPSETTING.

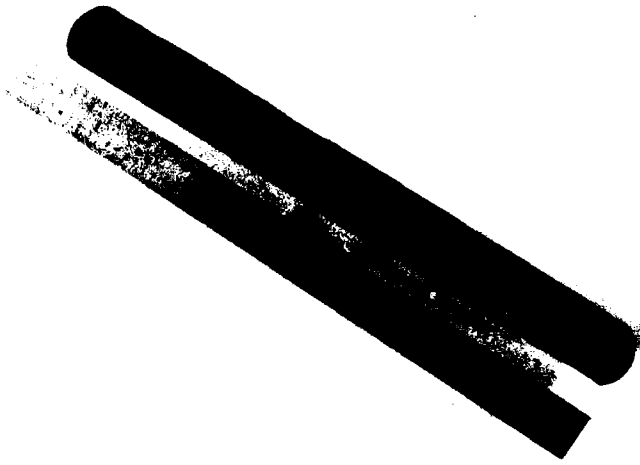


FIGURE 20. TRANSVERSE FORGED SPECIMEN 13, CROSS SECTION. MACROETCHED IN DILUTE NITRIC ACID.



FIGURE 21. DETAIL OF THE CENTER CROSS SECTION OF SPECIMEN 13 (FIGURE 20).

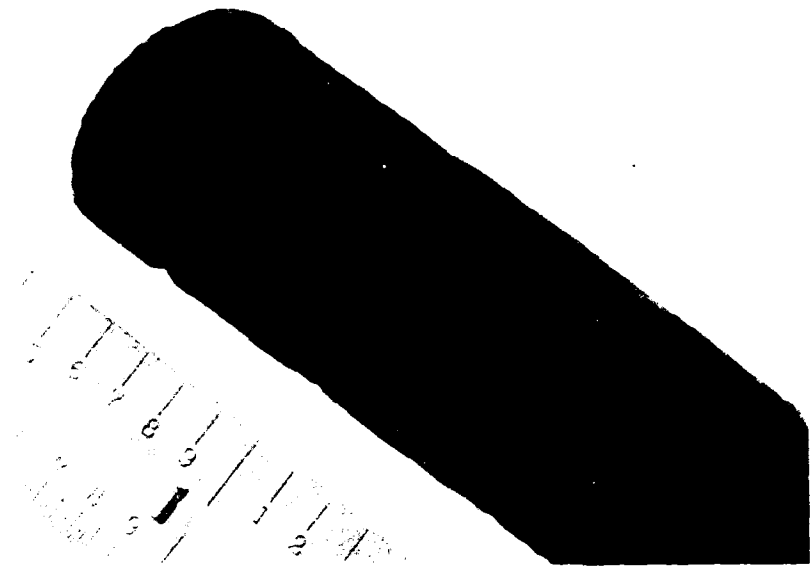
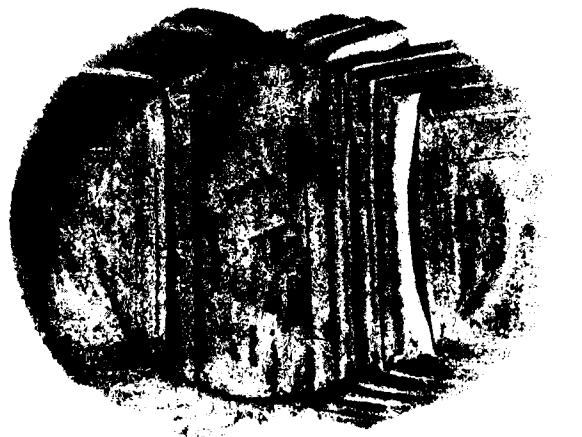


FIGURE 22. DETAIL OF THE EDGE CROSS SECTION OF SPECIMEN 13 (FIGURE 20).



10mm

FIGURE 23. TOP VIEW OF FORGEABILITY SPECIMEN 6A.

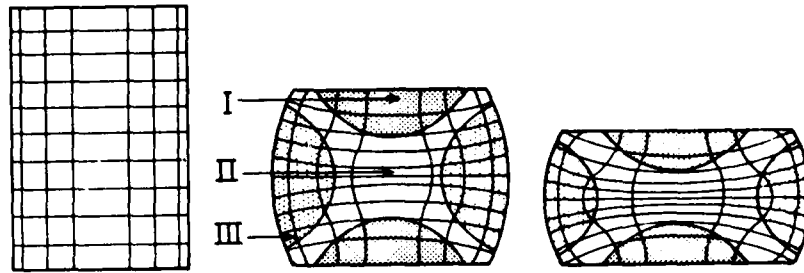


FIGURE 24. SCHEMATIC ILLUSTRATION OF INHOMOGENOUS DEFORMATION OF A CYLINDER DURING UPSETTING. AFTER REFERENCE 47.

material in contact with the forging die and the die itself, requiring lateral flow of metal near the die to proceed by shear alone without sliding. A top view of a buckled laminate cylinder is shown in Figure 23 in order to illustrate this frictional state. The lack of lateral material flow may be noted in this figure. In addition, the cross sectional morphology of the transverse forging shown in Figure 22 is a result of die friction and the anisotropy of lateral flow. During upsetting large tensile stresses are generated in the radial direction of the cylinder as a result of barrelling or non-homogeneous deformation. The barrelling itself is a consequence of the difficulty in flowing that the material adjacent to the die experiences as a result of friction, which, of course, inhibits outward flow directly, and local cooling of the specimen through conduction to the colder dies, which increases the flow stress of the cooler material. The consequences of these effects on the overall material flow in upsetting are illustrated schematically in Figure 24. Region I in this figure, the so-called "dead metal zone", remains nearly undeformed while most of the deformation occurs in Region II, which pushes outward deforming the material in Region III inhomogeneously. The morphological consequence of this flow is shown quite markedly in the transverse specimen cross section shown in Figure 20.

The phenomenon of hot or plastic buckling of the laminates observed for the laminates must be treated somewhat differently from that of barrelling. If each layer of the laminate cylinder is considered to be independent then the buckling of the plates is governed by a stability equation similar to Euler's column equation (pinned ends),⁴⁸

$$P_{cr} = \frac{\pi^2 EI}{L^2},$$

where

- P_{cr} = the critical load for buckling,
- E = the modulus of elasticity,
- I = the moment of inertia, and
- L = the column length (height),

in which the modulus, E , is replaced by a plastic modulus, E_t , that represents the slope of the stress strain curve in the plastic region at the stress value of interest.⁴⁹ The magnitude of E_t represents the work hardening capacity of the material, i.e., E_t for a perfectly plastic material would equal zero and would have no resistance to buckling after the yield strength had been exceeded. The moment of inertia for the lamina may be approximated by

$$I = \frac{bh^3}{12}$$

where

b = the plate (lamina) width and
h = the plate (lamina) thickness.

The critical load for buckling, of the lamina is, therefore,

$$P_{Cr} = \frac{\pi^2 E_t b h^3}{12L^2}$$

This equation then shows that the critical load is directly proportional to the plate width, the cube of thickness, and the plastic modulus or work hardening and inversely proportional to the square of the length or height. Since the interlaminar strength of these laminates is not zero, however, there must be an additional load required to separate them and the actual critical load must exceed P_{Cr} . Of course, if delamination did not obtain, then the laminate cylinder would be expected to barrel and deform continuously as do the monolithic cylinders. The fact that this does not happen is a result of die friction and the geometry of the individual laminae as explained below.

As noted previously the frictional condition for all the cylinder upset testing was one of essentially pure sticking friction and this allowed the modeling of the individual laminae as plates with pinned ends for the purpose of estimating buckling strength of each lamina. Since the laminae are not of equal width, however, their moments of inertia are not equal, the outer laminae being considerably less wide than the central layers (Figure 6b). In fact, the moment decreases as the chord of a circular section of the cylinder or as

$$b = 2(R^2 - d^2)^{1/2}$$

where

R = the cylinder radius and
d = the length of a normal from the layers to the center axis of the cylinder.

The buckling strength of the outer layers is, therefore, less than the central layers, and this leads to an inherent instability in the cylinders and favors delamination as the outer layers tend to buckle earlier and more than the

inner. This decrease in required buckling pressure is compensated partially, however, by the increase in pressure due to the die friction itself. Nevertheless, this pressure increases toward the center of the cylinder as $1/d$ and therefore, if sufficient pressure obtains at the outer layer for buckling, there will be adequate pressure on the inner as well, although along the plane perpendicular to the layers and passing through the cylinder axis the buckling is nearly stable, that is, delamination does not occur (Figure 25). Having established the instability of the laminate layers to buckling once they are decoupled, it is necessary to consider the development of cracking that leads to the decoupling and the actual buckling morphologies observed.

Delamination during upsetting is initiated primarily by the tensile stresses developed during the inhomogeneous deformation of the cylinders. As noted this inhomogeneity is itself a result of friction and local cooling of the forgings. The barrelling shown schematically in Figure 20 leads to very high tensile hoop stresses in Region III, indicated graphically by the divergence of the scribe lines as deformation progresses. These tensile hoop stresses lead to the onset of delamination in the laminate cylinders and to edge cracking in monolithic forgings. In the case of monolithic material, however, further cracking generally must be driven by the hoop stresses alone, whereas the laminate cylinders become unstable with respect to the alternative failure mode, buckling, as demonstrated above. It may be noted, in addition, that along the plane perpendicular to the layers and passing through the cylinder axis the buckling is almost stabilized and delamination does not occur between every layer as shown in Figure 25. This may also be explained by reference to Figure 20 since the radial stresses in Region II are essentially compressive and do not favor delamination. Furthermore, the dead metal zone, Region I, tends to shorten the effective or deforming lengths of the plates in the central region and increases the local buckling strength. It is illustrative that the onset of central delamination shown in the specimen of Figure 25 is at essentially the boundary of Regions II and III and that the layers within Region III have buckled almost stably, i.e., together, since the hoop stress is essentially in plane with them in this section and the plates have similar moments of inertia. The dead metal zone may also be perceived in cross section in Figure 25 and compared with the schematic in Figure 20. This final comparison can illustrate the explanation for the partially stable upset morphologies exhibited by some specimens and illustrated in Figure 19. In



10mm

FIGURE 25. CENTER PLANE SECTION OF SPECIMEN UP5B.
MACROETCHED IN NITRIC ACID. MAGNIFICATION: IX.

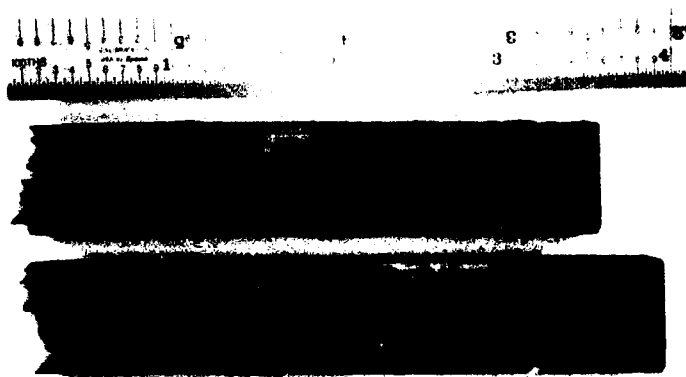


FIGURE 26. SIDE VIEW OF TRANSVERSE FORGING UP10 FRACTURED
TENSILE SPECIMEN SHOWING DELAMINATION AND
INDEPENDENT LAYER FRACTURE.

these specimens the dead metal zone sufficiently shortened the effective length of the central layers that they upset without gross buckling or completely delaminating. Nevertheless, sufficient local buckling and delamination did obtain in all cases to preclude the relevant tensile or fracture testing of this material.

3.2.1 Tensile Properties

The tensile properties of the base 300M plate and the base 4145 billet are listed in Tables 5 and 6, respectively, and the tensile properties of the 300M/1010 laminate as roll-bonded are listed in Table 7. Two comparisons are of primary note with respect to the 300M systems. First, the average strength, both tensile and ultimate, of the 300M/1010 laminate is less than the monolithic 300M. This is due to the fraction of lower strength interleaf material in the laminate. Since the volume fraction of 1010 is approximately 9.5 percent, the decrease in ultimate strength may be explained as a volume fraction effect by the rule of mixtures considering the tensile strength of the 1010 to be approximately 40 ksi (276 MPa). The decrease in yield strength, however, is greater than would be predicted by the rule of mixtures and appears to be a result of the plastic constraint imposed on the 300M layers following the yield of the 1010 interleaves. This leads to a biaxial tension-compression stress state in the layer or stronger material that reduces the apparent uniaxial yield strength.⁵⁰ Second, the average uniform elongation and true strain at necking of the laminate is slightly but consistently greater than the monolithic 300M. It is believed that this results from the stabilizing influence of multiple layers on flow, i.e., an incipient neck in one layer may be retarded from growing by the neighboring layers. This observation will be discussed further subsequently with respect to forged material and the interfacial strength of laminates.

As noted previously,^{35,36} the advantageous tensile and fracture properties of metal-metal laminates are a result of the independent behavior of the layers during fast fracture. This independence comes about through delamination of the layers because of the transverse tensile stresses developed by necking in the tensile test and plastic contraction in fracture toughness testing. In tension the laminate behaves elastically very much like the monolithic material and even after the weaker interleaves have yielded the contraction is insufficient to cause delamination up to the onset of necking. In

TABLE 5: TENSILE PROPERTIES OF 300M MONOLITH (PLATE)

SPECIMEN, HEAT TREATMENT, ORIENTATION	AVERAGE LAYER THICKNESS, in. (mm)	TRUE UPSET STRAIN, %	0.2% OFFSET YIELD STRENGTH, ksi (MPa)	ULTIMATE TENSILE STRENGTH, ksi (MPa)	TENSILE ELONGATION, %	UNIFORM ELONGATION, %	TRUE STRAIN AT NECKING, %	TRUE STRESS AT NECKING, ksi (MPa)
300M4, N, Q&T, L	---	0	220(1517)	250(1724)	12	4.0	3.9	268(1848)
300M5, N, Q&T, L	---	0	250(1724)	275(1896)	6.6	2.8	2.7	283(1951)
300M, N, Q&T, L AVERAGE	---	0	235(1620)	263(1813)	9.3	3.4	3.3	276(1903)

TABLE 6: TENSILE PROPERTIES OF 4145 BILLET

SPECIMEN, HEAT TREATMENT, ORIENTATION	AVERAGE LAYER THICKNESS, in. (mm)	TRUE UPSET STRAIN, %	0.2% OFFSET YIELD STRENGTH, ksi (MPa)	ULTIMATE TENSILE STRENGTH, ksi (MPa)	TENSILE ELONGATION, %	UNIFORM ELONGATION, %	TRUE STRAIN AT NECKING, %	TRUE STRESS AT NECKING, ksi (MPa)
4145,N,Q&T,L	---	0	234(1613)	275(1896)	9.0	3.3	3.2	284(1958)
4145,N,Q&T,L	---	0	224(1544)	265(1827)	6.3	3.2	3.1	273(1882)
4145,N,Q&T,L	---	0	223(1538)	259(1786)	4.6	2.4	2.3	265(1827)
4145,N,Q&T,L AVERAGE	---	0	227(1565)	266(1834)	6.6	3.0	2.9	274(1889)

TABLE 7: TENSILE PROPERTIES OF 300M/1010 LAMINATES AS ROLL-BONDED

SPECIMEN, HEAT TREATMENT, ORIENTATION	AVERAGE LAYER THICKNESS, in. (mm)	TRUE UPSET STRAIN, %	0.2% OFFSET YIELD STRENGTH, ksi (MPa)	ULTIMATE TENSILE STRENGTH, ksi (MPa)	TENSILE ELONGATION, %	UNIFORM ELONGATION, %	TRUE STRAIN AT NECKING, %	TRUE STRESS AT NECKING, ksi (MPa)
MM1,N,Q&T,L	0.122(3.10)	0	208(1434)	245(1689)	10	3.9	3.8	255(1758)
MM2,N,Q&T,L	0.135(3.43)	0	194(1338)	234(1613)	5.3	3.7	3.6	242(1669)
MM1,N,Q&T,L	0.155(3.94)	0	209(1441)	238(1641)	3.3	2.6	2.5	244(1682)
ZZ1,N,Q&T,L	0.118(3.00)	0	210(1448)	245(1689)	11	3.9	3.8	255(1758)
AS ROLLED AVERAGE	0.133(3.38)	0	205(1413)	241(1662)	7.5	3.5	3.4	249(1717)

fact, as noted above, the uniform elongation of the laminate is greater than the monolith. Following necking, however, the transverse stresses lead to delamination as shown in Figures 26-28 for a transversely forged specimen. The tensile data for the transversely forged specimens are listed in Table 8. The transverse forging of the as roll-bonded laminate did not significantly affect strength, although uniform elongation was improved significantly and tensile elongation was improved somewhat. This may be attributed to an improvement in the interlaminar bond integrity resulting from the increased transverse flow and compressive loading that obtains during forging. Following delamination during gross specimen necking each layer independently necks and finally fractures with each layer evincing a slant fracture. This independent behavior also means that the actual or total reduction in area for the laminate tensiles is greater, although the tensile elongation may not be significantly different. Finally, the strength of the forged laminate is indirectly related to the forging strain. This was noted only with respect to the UP11 forging, however, and resulted from the accidental forging of a section of the 1010 steel box used during roll bonding into the forging. There was, therefore, a large volume fraction of lower strength material in this specimen. The subject of post-forged tensile properties will be discussed in greater detail subsequently after the presentation of the closed die or complex flow forging data.

3.2.2 Micrography

The microstructure of the transverse forgings in the quenched and tempered condition was not significantly altered versus the as roll-bonded laminate as shown in Figure 29. In general, the density of small voids at the bond line decreases after forging, compare Figure 13, and the spheroidite free zone disappears, of course, in the heat treated condition. It may be noted that the lighter gray fine tempered martensite does penetrate beyond the small voids and into the interleaf. This is probably a result of the diffusion of alloying elements into the low carbon interleaf, thereby improving its hardenability. The microstructure of the interleaf is mixed pearlitic, bainitic, and martensitic.

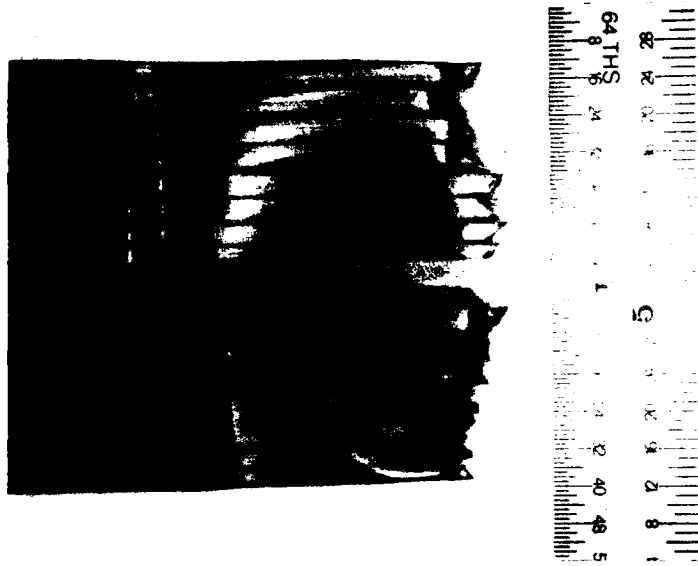


FIGURE 27. DETAIL OF THE SPECIMEN OF FIGURE 26.

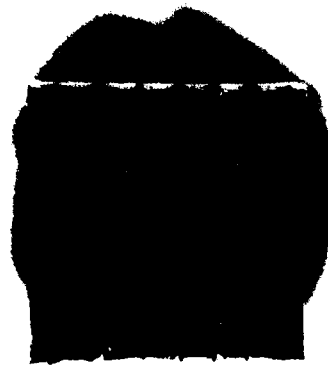
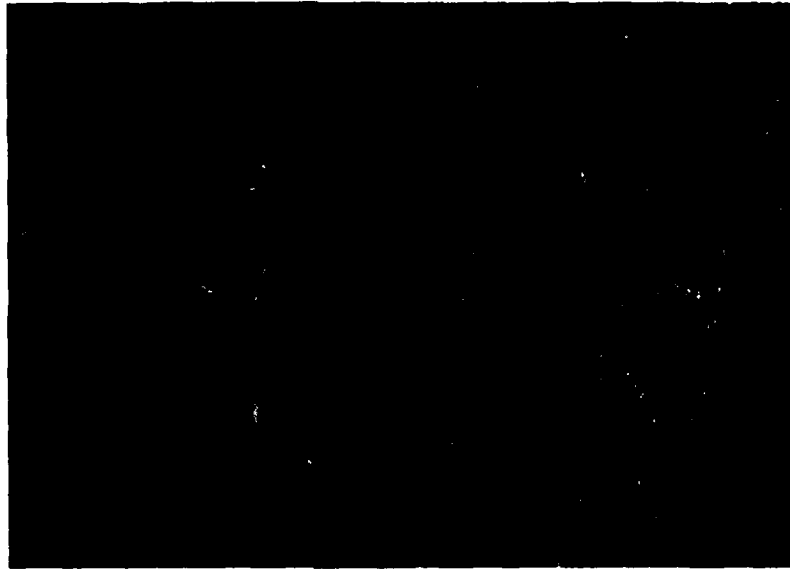


FIGURE 28. TOP VIEW OF THE FRACTURE SURFACES OF A TENSILE SPECIMEN MACHINED FROM TRANSVERSE FORGING UP10.

TABLE 8: TENSILE PROPERTIES OF 300M/1010 LAMINATES FORGED TRANSVERSELY

SPECIMEN, HEAT TREATMENT, ORIENTATION	AVERAGE LAYER THICKNESS, in. (mm)	TRUE UPSET STRAIN, %	0.2% OFFSET YIELD STRENGTH, ksi (MPa)	ULTIMATE TENSILE STRENGTH, ksi (MPa)	TENSILE ELONGATION, %	UNIFORM ELONGATION, %	TRUE STRAIN AT NECKING, %	TRUE STRESS AT NECKING, ksi (MPa)
UP10,N,Q&T,T	0.072(1.83)	38.3	211(1765)	256(1765)	10	5.3	5.1	270(1862)
UP10,N,Q&T,L	0.074(1.88)	38.3	216(1489)	258(1779)	9.7	5.0	4.9	271(1869)
UP11,N,Q&T,T	0.046(1.17)	55.7	173(1193)	206(1420)	9.5	5.3	5.1	217(1496)
UP11,N,Q&T,L	0.049(1.25)	55.7	195(1345)	233(1607)	8.7	4.9	4.8	244(1682)



100 μm

FIGURE 29. MICROGRAPH OF TRANSVERSE FORING UPI0, TRANSVERSE SECTION. THE 1010 INTERLEAF IS AT THE LEFT. MAGNIFICATION: 200X. 2% NITAL ETCHANT.

3.2.3 Fracture Properties

The fracture toughness data for the baseline 300M plate and 4145 billet are listed in Tables 9 and 10, respectively. The important values for subsequent comparison are the average toughnesses and strength ratios. It is also worthy of note that the monolithic toughness of the 300M plate is generally slightly greater in the LT orientation. The highest toughness orientation for the 4145 billet is the TS orientation. Since the toughness versus thickness relationship was of importance for the 300M, several thicknesses were tested, all of the LT orientation. For comparison and baseline purposes the fracture toughness of the as roll-bonded 300M/1010 laminate was determined and these results are listed in Table 11. Similar comparison results may also be found in Reference 35. Although the plane strain average or conditional fracture toughness of the laminate is somewhat greater than equivalent monolithic material, the significant effect of lamination is best seen through comparison of the critical fracture toughness, an elastic-plastic toughness, that measures the resistance of the material to fast fracture or critical crack growth more effectively than the conditional toughness. Since the individual layers in the laminate would not meet ASTM E 399³⁷ criteria for K_{Ic} , the term conditional fracture toughness is used for both laminate and monolithic material. It may also be noted that the laminate strength ratios are much higher than the monolithic alloy. This increase in toughness in the laminate comes about because the individual layers decouple near the onset of unstable crack propagation and in thick laminates the stress state changes from one of essentially pure plane strain closer to one of plane stress. This individual layer behavior may be seen in the compact tension specimen shown in Figure 30. Note that the fatigue precrack fracture surface is flat and that shear lips are not developed until fast fracture commences. In fact, it has been fractographically determined in previous work by the author³⁶ that the delamination does not occur until there is sufficient plastic contraction, that is within the stretch zone. As a result of this decoupling the required critical fracture toughness or energy for fast fracture is greatly enhanced.

The effect of forging on the fracture toughness of both the 300M/1010 laminate and the 4145 cylinders may be evaluated through reference to Tables 12 and 13. The toughness results for the 4145 forgings that are listed in Table 12 are somewhat higher in general than those for the 4145 billet (Table 10).

TABLE 9: FRACTURE TOUGHNESS OF 300M MONOLITH (PLATE)

SPECIMEN HEAT TREATMENT, ORIENTATION	AVERAGE LAYER THICKNESS, in. (mm)	TOTAL THICKNESS, in. (mm)	TRUE UPSET STRAIN, %	CONDITIONAL FRACTURE TOUGHNESS, ksi-in. ^{1/2} (MPa-m ^{1/2})	APPARENT FRACTURE TOUGHNESS, ksi-in. ^{1/2} (MPa-m ^{1/2})	CRITICAL FRACTURE TOUGHNESS, ksi-in. ^{1/2} (MPa-m ^{1/2})	SPECIMEN STRENGTH RATIO
300M,N,Q&T,LT	---	0.742(18.85)	0	72.8(80.0)	72.9(80.1)	81.7(89.8)	0.451
300M,N,Q&T,TL	---	0.742(18.85)	0	69.2(76.0)	69.5(76.4)	72.3(79.4)	0.396
300M,N,Q&T,LT	---	0.541(13.74)	0	72.5(79.7)	73.2(80.4)	82.4(90.5)	0.406
300M,N,Q&T,LT	---	0.538(13.67)	0	58.0(63.7)	58.0(63.7)	58.0(63.7)	0.346
300M,N,Q&T,LT	---	0.285(7.24)	0	72.7(79.9)	76.7(84.3)	101(111)	0.474
300M,N,Q&T,LT	---	0.145(3.68)	0	81.3(89.3)	91.7(101)	135(148)	0.621
300M,N,Q&T,LT	---	0.144(3.66)	0	81.7(89.8)	90.7(100)	123(135)	0.615
300M,N,Q&T,LT PLANE STRAIN AVERAGE	---	0.607(15.42)	0	67.8(74.5)	68.0(74.7)	74.0(81.3)	0.401

TABLE 10: FRACTURE TOUGHNESS OF 4145 BILLET

SPECIMEN HEAT TREATMENT, ORIENTATION	AVERAGE LAYER THICKNESS, in. (mm)	TOTAL THICKNESS, in. (mm)	TRUE UPSET STRAIN, %	CONDITIONAL FRACTURE TOUGHNESS, ksi-in. ^{1/2} (MPa-m ^{1/2})	APPARENT FRACTURE TOUGHNESS, ksi-in. ^{1/2} (MPa-m ^{1/2})	CRITICAL FRACTURE TOUGHNESS, ksi-in. ^{1/2} (MPa-m ^{1/2})	SPECIMEN STRENGTH RATIO
4145, N, Q&T, LT	---	0.379(9.63)	0	30.0(33.0)	31.1(34.2)	37.7(41.4)	0.218
4145, N, Q&T, TL	---	0.588(14.94)	0	28.5(31.3)	28.9(31.8)	32.3(35.5)	0.203
4145, N, Q&T, TS	---	0.725(18.42)	0	45.3(49.8)	45.7(50.2)	50.7(55.7)	0.298
4145, N, Q&T, TS	---	0.705(17.91)	0	41.7(45.8)	41.9(46.0)	42.9(47.1)	0.292
4145, N, Q&T, ST	---	0.576(14.63)	0	35.1(38.6)	37.2(40.9)	39.7(43.6)	0.334
4145, N, Q&T, SL	---	0.465(11.81)	0	29.8(32.7)	30.3(33.3)	36.6(40.2)	0.243
4145, N, Q&T, ALL AVERAGE	---	0.573(14.55)	0	35.1(38.6)	35.9(39.4)	40.0(44.0)	0.265

TABLE 11: FRACTURE TOUGHNESS OF 300M/1010 LAMINATES AS ROLL-BONDED

SPECIMEN HEAT TREATMENT, ORIENTATION	AVERAGE LAYER THICKNESS, in. (mm)	TOTAL THICKNESS, in. (mm)	TRUE UPSET STRAIN, %	CONDITIONAL FRACTURE TOUGHNESS, ksi-in. ^{1/2} (MPa-m ^{1/2})	APPARENT FRACTURE TOUGHNESS, ksi-in. ^{1/2} (MPa-m ^{1/2})	CRITICAL FRACTURE TOUGHNESS, ksi-in. ^{1/2} (MPa-m ^{1/2})	SPECIMEN STRENGTH RATIO
MM1, N, Q&T, LT	0.129(3.28)	0.443(11.25)	0	79.9(87.8)	93.0(102)	164(180)	0.808
MM2, N, Q&T, LT	0.133(3.38)	0.501(12.73)	0	59.4(65.3)	77.0(84.6)	179(197)	0.768
MM3, N, Q&T, LT	0.120(3.05)	0.685(17.40)	0	81.9(90.0)	91.0(100)	145(159)	0.793
MM4, N, Q&T, LT	0.139(3.53)	0.664(16.87)	0	84.9(93.3)	94.7(104)	141(155)	0.727
MM, NQ&T, LT AVERAGE	0.130(3.30)	0.573(14.55)	0	76.5(84.1)	88.9(97.7)	157(173)	0.774



(a)



(b)

FIGURE 30. 300M/1010 LAMINATE COMPACT TENSION SPECIMEN
MM3 FRACTURE SURFACES. (a) TOP VIEW,
(b) END VIEW.

TABLE 12: FRACTURE TOUGHNESS OF 4145 UPSET FORGINGS

SPECIMEN HEAT TREATMENT, ORIENTATION	AVERAGE LAYER THICKNESS, in. (mm)	TOTAL THICKNESS, in. (mm)	TRUE UPSET STRAIN, %	CONDITIONAL FRACTURE TOUGHNESS, ksi-in. ^{1/2} (MPa-m ^{1/2})	APPARENT FRACTURE TOUGHNESS, ksi-in. ^{1/2} (MPa-m ^{1/2})	CRITICAL FRACTURE TOUGHNESS, ksi-in. ^{1/2} (MPa-m ^{1/2})	SPECIMEN STRENGTH RATIO
UP7A, N, Q&T, LT (MID)	---	0.414(10.52)	42.9	40.9(44.9)	41.2(45.3)	43.7(48.0)	0.267
UP7A, N, Q&T, LT (TOP)	---	0.538(13.67)	42.9	42.8(47.0)	43.0(47.3)	46.1(50.7)	0.297
UP8A, N, Q&T, SL	---	0.621(15.77)	45.9	52.3(57.5)	52.3(57.5)	55.4(60.9)	0.359
UP9A, N, Q&T, LT (TOP)	---	0.396(10.06)	78.9	47.0(51.6)	47.9(52.6)	54.9(60.3)	0.317

TABLE 13: FRACTURE TOUGHNESS OF 300M/1010 LAMINATES FORGED TRANSVERSELY

SPECIMEN HEAT TREATMENT, ORIENTATION	AVERAGE LAYER THICKNESS, in. (mm)	TOTAL THICKNESS, in. (mm)	TRUE UPSET STRAIN, %	CONDITIONAL FRACTURE TOUGHNESS, ksi-in. ^{1/2} (MPa-m ^{1/2})	APPARENT FRACTURE TOUGHNESS, ksi-in. ^{1/2} (MPa-m ^{1/2})	CRITICAL FRACTURE TOUGHNESS, ksi-in. ^{1/2} (MPa-m ^{1/2})	SPECIMEN STRENGTH RATIO
UP10,N,Q&T,LT	0.060(1.52)	0.727(18.47)	48.2	36.2(94.7)	104(114)	205(225)	1.05
UP10,N,Q&T,LT	0.075(1.91)	0.681(17.30)	48.2	>70.2(77.1)*	---	---	---
UP10,N,Q&T,TL	0.080(2.03)	0.684(17.37)	48.2	91.5(101)	109(120)	200(220)	1.10
UP11,N,Q&T,TL	0.056(1.42)	0.625(15.88)	81.5	---	---	>188(207)+	---
UP12,N,Q&T,LT	0.052(1.32)	0.472(11.99)	86.7	145(159)	153(168)	194(213)	1.209
UP12,N,Q&T,TL	0.051(1.30)	0.466(11.84)	86.7	111(122)	129(142)	225(247)	1.271
UP13,N,Q&T,LT	0.046(1.17)	0.479(12.17)	101	110(121)	127(140)	219(230)	1.208
UP13,N,Q&T,TL	0.043(1.09)	0.487(12.37)	101	109(120)	128(141)	228(251)	1.272

*TESTING MACHINE MALFUNCTION

+SPECIMEN OVERLOADED DYNAMICALLY

This improvement is a result of the additional flow or fiber developed during upsetting, and both of the specimen orientations tested, i.e., LT and SL, are of the high toughness "cross grain" type. Some improvement in toughness in the LT orientation may also be noted with increasing upset strain as the flow and fiber in this orientation is further refined. There was also a slight difference between the top and mid-plane toughness in forging 7A in the LT orientation, although this is not considered significant and probably arises from slight orientational differences with respect to the fiber of the upset cylinder.

The fiber of metal-metal laminates on the other hand is intrinsically determined by the arrangement of the laminae. Since laminate transverse forgings flow in the two directions of the lamellar planes the LT orientation remains rigorously "cross grain" or cross fiber in these forgings as it was in the parent laminate plate. The consistently improved toughness of the transverse laminate forgings may be appreciated by comparing Table 13 with Table 11. Since the fiber orientation between all these specimens is the same, however, the improved toughness must result from flow or other geometric differences. In fact, the primary improvement in toughness is a result of the thinner layers in the forged laminate, which shifts the decoupled stress state further toward the tougher plane stress condition, note Figure 4. The subject of layer thickness versus toughness will be discussed in greater detail subsequently.

3.3 COMPLEX FLOW EVALUATION (CLOSED DIE FORGING)

The metal laminate cylinders forged in a closed die to form the part shown in Figure 7 demonstrated excellent forgeability in this complex flow geometry both with respect to the stability of the layer versus interleaf flow and the ability to flow in three dimensions, that is perpendicular to the lamellar plane. In addition, the intrinsic fiber of the laminate acted as an extremely effective tracer for the flow patterns developed during the closed die forging of the part geometry investigated. The as forged appearance of the first closed die forging (CD1) is shown in Figure 31. The uneven edge material in this forging is flash and some delamination of the laminate did obtain in the flash as may be noted in the figure. Nevertheless, the material flowed very well and stably as shown in the cross section of CD1 reproduced in Figure 32.

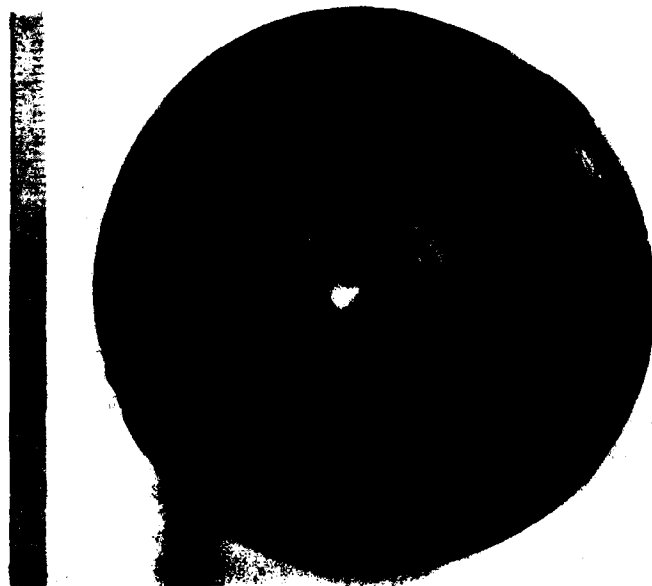


FIGURE 31. CLOSED DIE FORGING CDI.
TOP VIEW.



FIGURE 32. RADIAL CROSS SECTION OF CLOSED DIE FORGING CDI.
MACROETCHED IN NITRIC ACID.

The flow is illustrated very well in this figure including the reversal of flow that occurs in the outer flange as the flowing steel reaches the flash gutter of the die. The delamination that developed between the sixth and seventh layers from the top extended approximately one inch into the forging at this point. This delamination developed as the material began to flow into the flange section as shown in Figures 33 and 34 of forging CD2. This forging did not fill the die but rather stopped flowing just after the material had reached the flange cavity and begun to spread. The tensile stresses developed as a result of die friction as the forging began to flow into the flange cavity were sufficient to cause delamination. Although these delaminations may shut during subsequent die filling they will usually result in seams as shown in Figure 32. Whenever the stress state is basically compressive, however, as it is in the hub cavity of the die, the dual metal laminate flows stably without separation of layers and interleaves. This may be seen quite well in the etched cross sections shown in Figures 32 and 34. The closed die forging, complex flow evaluation may be considered to give rise to a flow and stress state intermediate between that encountered in the longitudinal and transverse open die forging. The successful forging of laminates in a closed die are contingent upon proper die design in which flow, particularly divergent flow such as that into the flange cavity, is prevented or inhibited through the use of generous billet radii and draft.

3.3.1 Micrography

Representative microstructures from the web area of a closed die forging are shown in Figures 35-37. In general, the flow obtaining during forging appears to improve the integrity of the layer-interleaf bond as notable in Figure 37. The excellent stability of the flow is also markedly illustrated in the low magnification micrograph of Figure 35. The flow stability of laminates is the second most important criterion for the successful forging of these materials, the primary one being a basically compressive stress state perpendicular to the lamellar plane. Even at the very high strains, -107 percent to -154 percent, produced during the closed die forging, however, the layer and interleaf materials deformed almost uniformly and stably. Such stable deformation appears to be primarily contingent upon the existence of

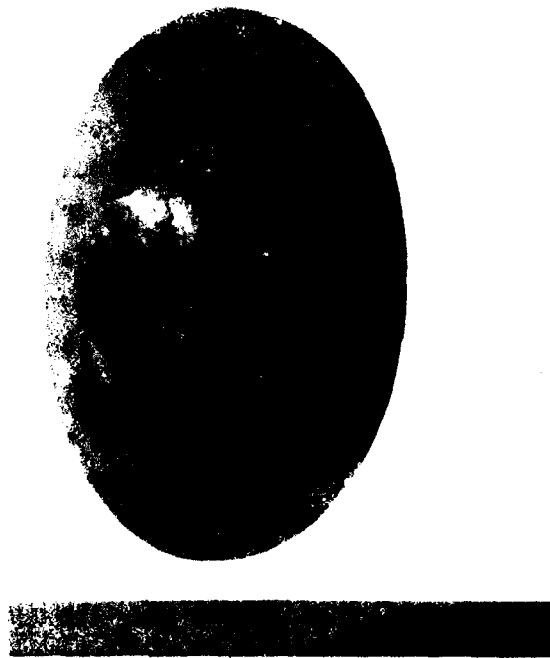


FIGURE 33. THREE QUARTERS VIEW OF CLOSED DIE FORGING CD2 AS FORGED.



FIGURE 34. RADIAL CROSS SECTION OF CLOSED DIE FORGING CD2. MACROETCHED IN NITRIC ACID.

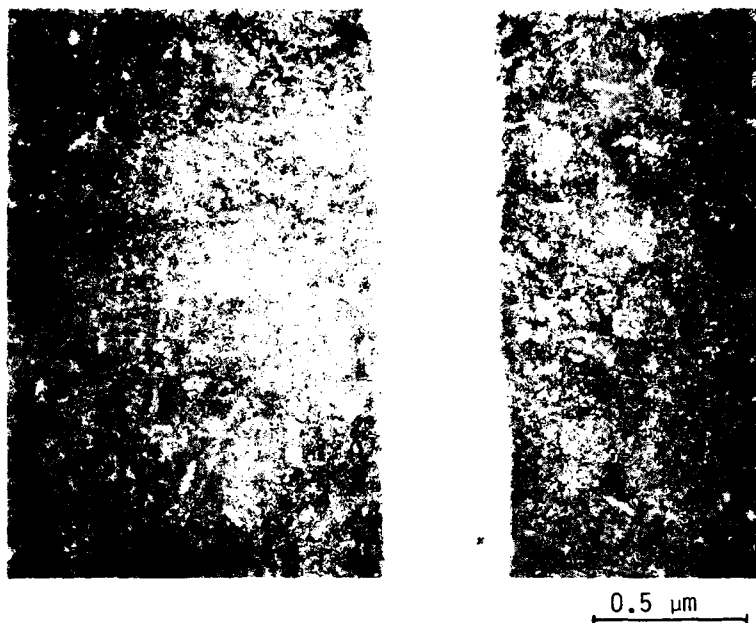


FIGURE 35. MICROGRAPH OF CLOSED DIE FORGING CD3, TRANSVERSE SECTION. MAGNIFICATION: 44X. 2% NITAL ETCHANT.

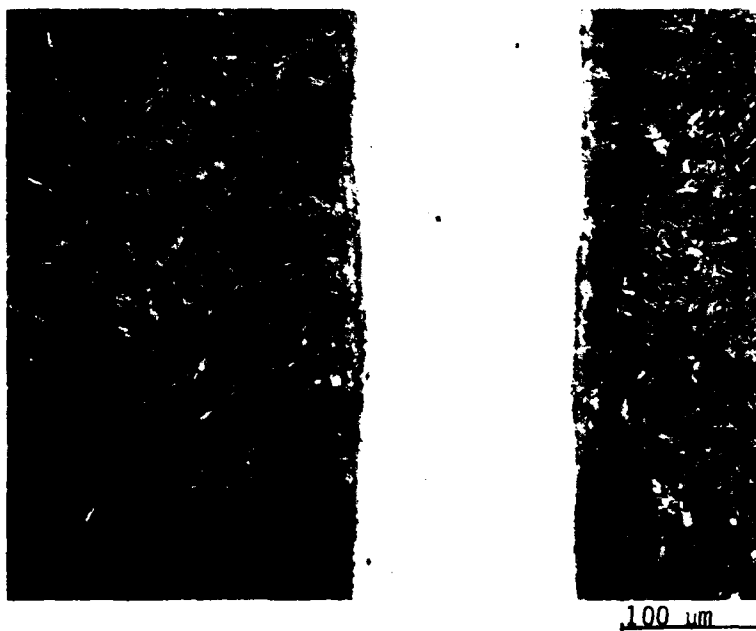


FIGURE 36. DETAIL OF FIGURE 35. MAGNIFICATION: 500X. 2% NITAL ETCHANT.



FIGURE 37. DETAIL OF FIGURE 35. THE 1010 INTERLEAF IS AT THE RIGHT. MAGNIFICATION: 500X. 2% NITAL ETCHANT.

approximately equal flow stresses in the two materials at the operational deformation temperature. Previous unpublished work by the author on the hot deformation of the beta titanium alloys suggests that the material with the higher flow stress will tend to breakup or fragment during deformation. This is also in agreement with earlier work by Semiatin and Piehler⁵¹ on the room temperature deformation of clad sheet materials in rolling.

The microstructural transformation products of the closed die forgings are similar to the other heat treated laminates with the exception of less proeutectoid product appearing in the 1010. Since these structures are representative of the relatively thin web, the 1010 interleaf is nearly completely transformed to a bainite, while the 300M is tempered martensite as expected. The line of demarcation between the martensitic and bainitic structures is once again quite clear, although the few lighter etching patches in the 300M near this line may be evidence of the original bondline as discussed in Section 3.1.1. The relatively larger prior austenite grain size and wide grain size variation is probably a remnant of the rather high, 2400°F (1316°C), forging temperature used.

3.3.2 Tensile Properties

The tensile properties of the several closed die forgings tested are listed in Table 14. A comparison of these results with Tables 7 and 8 will reveal that, in general, both the tensile strength and yield strength of the closed die laminates is lower than the as roll-bonded or transversely forged laminate. This effect is illustrated in Figure 38 in which the strength is plotted versus strain for the various material systems. The tensile strength of the closed die forging is, in fact, less than that predicted by the rule of mixtures and suggests either a difference in the intrinsic strength of the 300M layers in these forgings or a change based on the structural differences, such as the thinner layers and interleaves and the improved bond. It is felt that the latter, structural differences, are probably more instrumental in this regard for the following reasons. First, although the volume fraction is approximately the same, the thinner layers are more effectively stressed, i.e., a greater fraction of each layer is affected, by the plastic contraction of the interleaf as discussed in Section 3.2.1. Second, as a result of the improved bond integrity this traction is continued to higher levels of tensile

TABLE 14: TENSILE PROPERTIES OF 300M/1010 LAMINATE CLOSED DIE FORGINGS

SPECIMEN, HEAT TREATMENT, ORIENTATION	AVERAGE LAYER THICKNESS, in. (mm)	TRUE UPSET STRAIN, %	0.2% OFFSET YIELD STRENGTH, ksi (MPa)	ULTIMATE TENSILE STRENGTH, ksi (MPa)	TENSILE ELONGATION, %	UNIFORM ELONGATION, %	TRUE STRAIN AT NECKING, %	TRUE STRESS AT NECKING, ksi (MPa)
CU3, N, Q&T, T*	0.047(1.19)	107	86.7(597.8)	134(923.9)	---	---	---	---
CU3, N, Q&T, T*	0.047(1.19)	107	---	112(722.2)	---	---	---	---
CU4, N, Q&T, T	0.025(0.64)	154	197(1358)	237(1634)	9.8	5.1	5.0	249(1717)
CU3, N, Q&T, T	0.034(0.86)	154	190(1310)	233(1606)	7.5	3.8	3.7	241(1662)
CU4, N, Q&T, T	0.030(0.76)	154	194(1338)	235(1620)	8.7	4.5	2.9	245(1689)
AVERAGE								
CU5, N, Q&T, T	0.030(0.76)	152	196(1351)	226(1558)	9.5	5.5	5.4	239(1648)
CU5, N, Q&T, T	0.030(0.76)	152	190(1310)	233(1606)	7.5	3.8	3.7	241(1662)
CU5, N, Q&T, T	0.030(0.76)	152	194(1338)	235(1620)	9.2	4.8	4.6	247(1703)
CU5, N, Q&T, T AVERAGE	0.030(0.76)	152	194(1338)	232(1600)	8.7	4.7	4.6	242(1669)

*FAILED AT LAMINATE INTERFACE

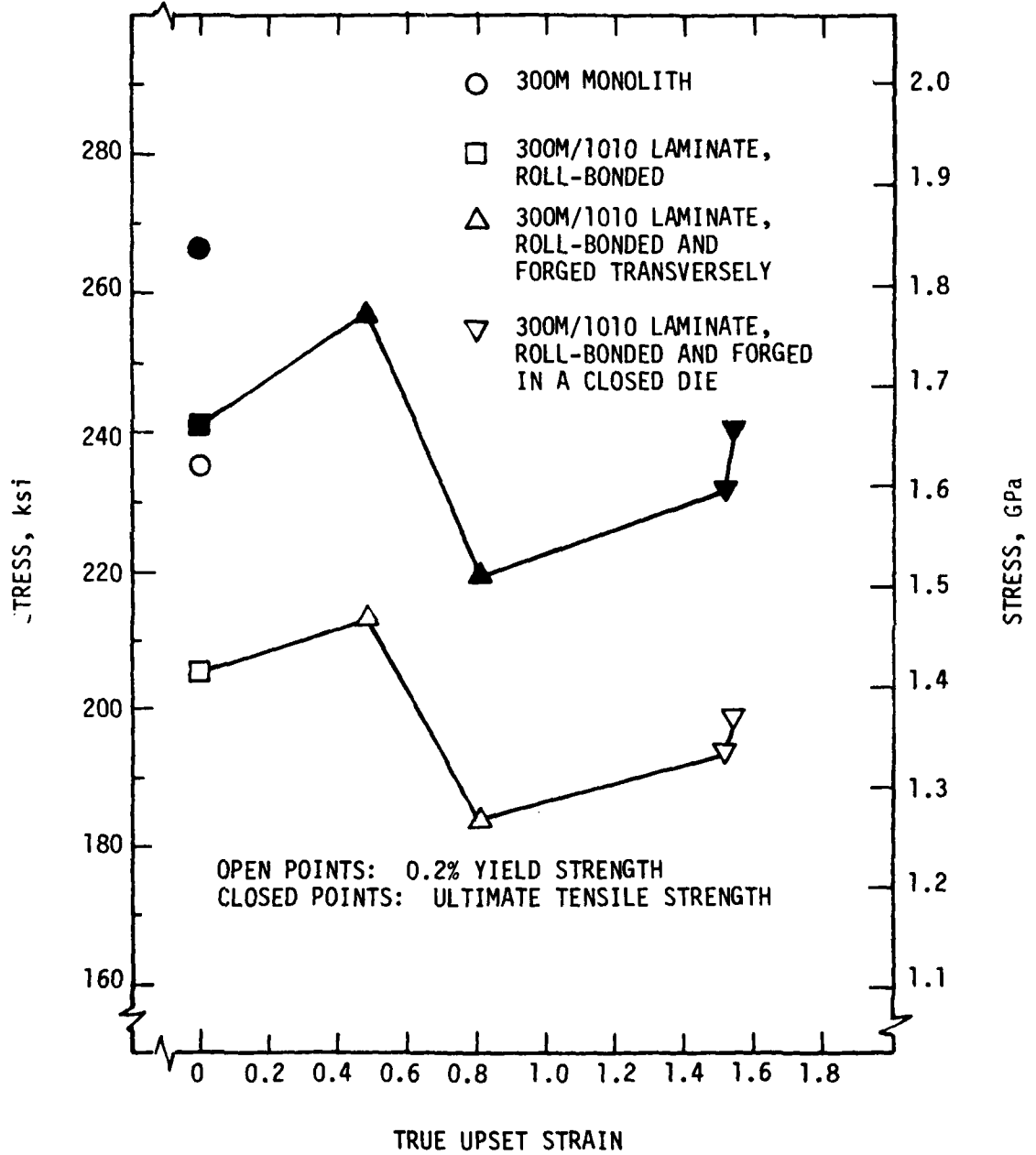


FIGURE 38. YIELD AND TENSILE STRENGTH VERSUS UPSET STRAIN FOR THE 300M MONOLITHIC AND 300M/1010 LAMINATE SYSTEMS.

elongation, thereby further depressing the ultimate tensile strength for all forged material versus the as roll-bonded laminate. That this greater elongation did obtain for the forgings is demonstrated by the data of Figure 39 in which elongation is plotted versus upset strain. In this figure the trend toward improved uniform elongation in laminates noted previously^{35,36} is demonstrated very well. Although it is somewhat speculative at this point, it is felt that an optimum layer-interleaf bond strength may exist for the best combination of strength and tensile ductility or formability, since uniform elongation may be correlated well with formability in many alloy systems.⁵² Previous tensile results reported by Johnson³³ for a Ti-6Al-4V/CP titanium laminate in which delamination did not occur suggest to the current author that it is possible to obtain a system for which the bond strength is too great for individual layer behavior either in tension or in sharp crack fracture testing. This, then, leads to laminate behavior that is indistinguishable from the monolithic. The consequences of this more monolithic behavior are reflected in the decreasing total elongation with improved bond strength as displayed in Figure 39. Nevertheless, the laminae did behave independently in tensile fracture even in the most severely deformed closed die forging. This is illustrated in Figures 40 and 41. Once again the actual reduction in area of the laminate is much greater than a corresponding monolithic material since each layer necks individually. It may also be noted in Figures 40 and 41 that as the layer thickness is decreased the individual layers begin to behave more as if they were thin sheets, i.e., their tensile elongation is truncated vis à vis thick specimens following necking,⁵³ and this may also contribute to the decreased total elongation of the laminates with increased upset strain. Finally, because of the different thermal-mechanical history of the closed die forgings, especially the high forging temperature, some variability in their tensile properties may be an effect of metallurgical condition, although this effect is almost certainly very secondary to the consequences of the structural differences.

3.3.3 Fracture Properties

The fracture toughness properties of the closed die forgings listed in Table 15 are in general agreement with the statement that the toughness, especially the critical fracture toughness, improves with decreasing layer

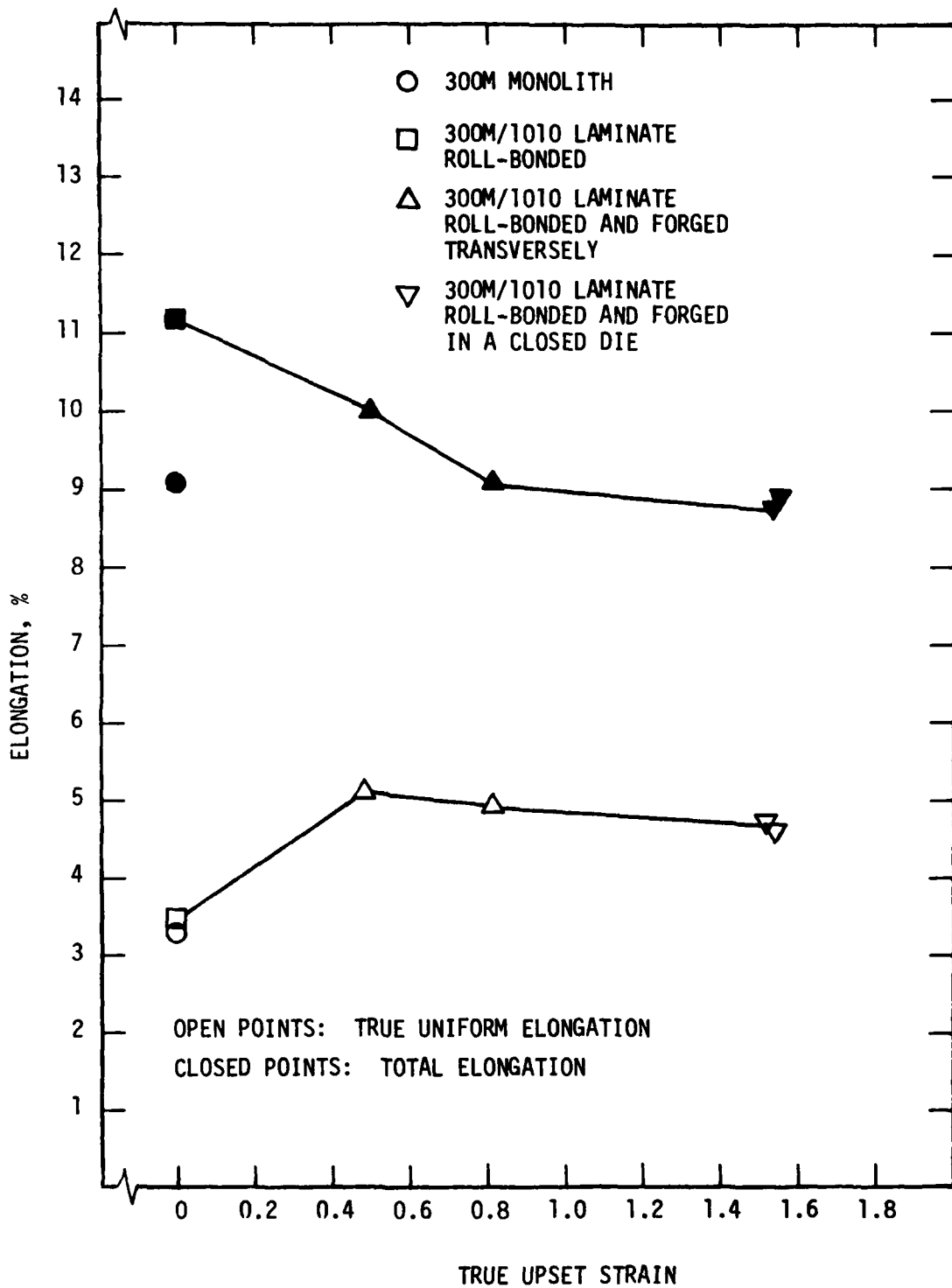


FIGURE 39. UNIFORM AND TOTAL TENSILE ELONGATION VERSUS UPSET STRAIN FOR THE 300M MONOLITHIC AND 300M/1010 LAMINATE SYSTEMS.

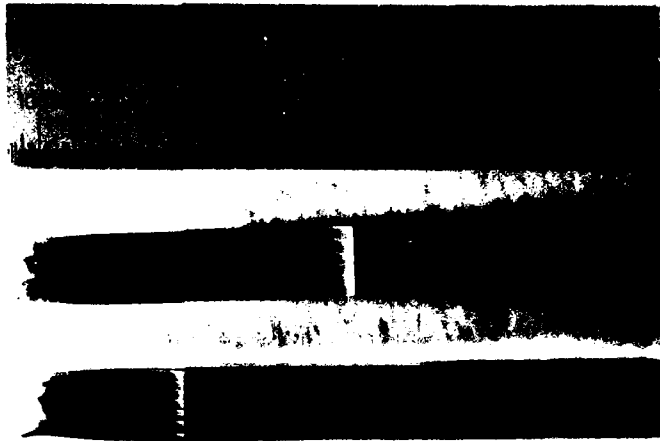


FIGURE 40. SIDE VIEW OF A FRACTURED TENSILE SPECIMEN MACHINED FROM CLOSED DIE FORGING CD5.

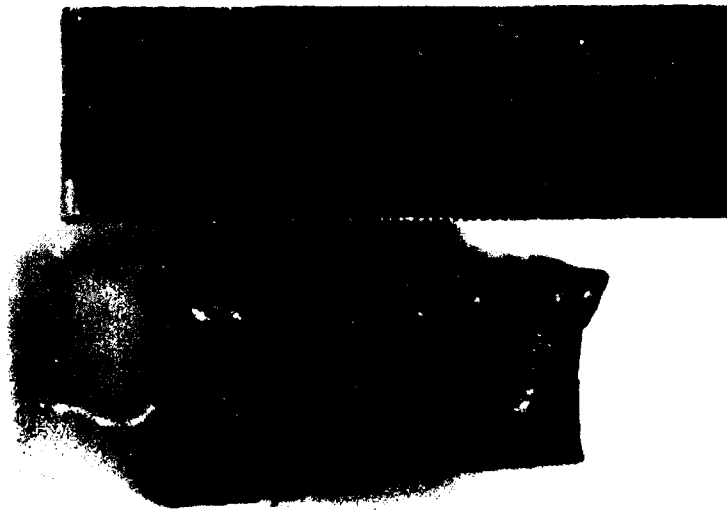


FIGURE 41. VIEW OF THE MATING TENSILE FRACTURE SURFACES OF CLOSED DIE FORGING CD5.

thickness. Nevertheless, a comparison of Table 15 with Table 13 will reveal that the transversely forged laminates were somewhat tougher across the spectrum than the closed die forgings. This is believed to result from the improved bond strength of the closed die forged material. Such improved strength would lead to a delay in the onset of delamination and the imposition of a greater triaxial component during fast fracture giving rise to a more plane strain condition and consequently lower toughness. Nevertheless, the individual layers still do delaminate and fail in mixed mode as shown in Figure 42. In addition to the improved bond strength, the wavy or non-linear character of the layers and their uneven thicknesses may have affected toughness, although it is not felt that this would have been sufficient to have accounted for a significant fraction of the observed difference in toughness. Rather it is more probable that with regard to the toughness as well as the tensile ductility (See previous section.) there is an optimum level of bond strength.

3.4 GENERAL DISCUSSION OF LAMINATE FRACTURE TOUGHNESS

As pointed out previously above and in other publications^{4,34,35,36} the two primary criteria for improved fracture toughness in metal-metal laminates are (1) a thin layer thickness in which plane strain conditions do not obtain and (2) the mechanical decoupling of the layers during fast fracture. It has also been demonstrated previously³⁵ that when these conditions obtain without qualification the thin layer toughness may be maintained in laminate panels of indefinite thickness. This is demonstrated well by plotting the critical toughness, an elastic-plastic parameter, for the 300M/1010 laminates in all conditions versus the toughness of monolithic 300M of the same heat treatment as has been done in Figure 43. With the exception of the one transversely forged datum, representing a testing machine malfunction, the toughness of the laminates is maintained at mixed mode, i.e., between plane strain and plane stress levels even in panel thicknesses at which the usual plane strain criteria would be expected to apply. The line plotted to represent the laminate K_{IC} is a simple least squares⁵⁴ fit to all the laminate data excluding the one outlying point. The line represents essentially no correlation between toughness and panel thickness. Most of the scatter notable in the laminate data of Figure 43 may be removed, in fact, by replotting the same

TABLE 15: FRACTURE TOUGHNESS OF 300M/1010 LAMINATE CLOSED DIE FORGINGS

SPECIMEN HEAT TREATMENT, ORIENTATION	AVERAGE LAYER THICKNESS, in. (mm)	TOTAL THICKNESS, in. (mm)	TRUE UPSET STRAIN, %	CONDITIONAL FRACTURE TOUGHNESS, ksi-in. ^{1/2} (MPa-m ^{1/2})	APPARENT FRACTURE TOUGHNESS, ksi-in. ^{1/2} (MPa-m ^{1/2})	CRITICAL FRACTURE TOUGHNESS, ksi-in. ^{1/2} (MPa-m ^{1/2})	SPECIMEN STRENGTH RATIO
CU3, N, Q&T, LT	0.047(1.19)	0.555(14.10)	107	78.1(85.9)	95.4(105)	193(212)	0.960
CU3, N, Q&T, TL	0.038(0.97)	0.574(14.58)	107	71.1(78.2)	88.7(97.6)	187(206)	0.911
CU4, N, Q&T, LT	0.034(0.86)	0.290(7.37)	154	70.0(77.0)	88.2(97.0)	183(201)	0.909
CU4, N, Q&T, TL	0.025(0.64)	0.281(7.14)	154	80.1(88.1)	96.3 (106)	190(209)	0.925
CU5, N, Q&T, LT	0.030(0.76)	0.280(7.11)	152	85.1(93.6)	101 (111)	166(183)	0.952
CU5, N, Q&T, TL	0.030(0.76)	0.280(7.11)	152	84.9(93.4)	99.0 (109)	178(196)	0.940
CU, N, Q&T, LT AVERAGE	0.037(0.94)	0.375(9.53)	138	77.7(85.5)	94.9 (104)	181(199)	0.940
CU, N, Q&T, TL AVERAGE	0.031(0.79)	0.378(9.60)	138	78.7(86.6)	94.7 (104)	185(203)	0.925

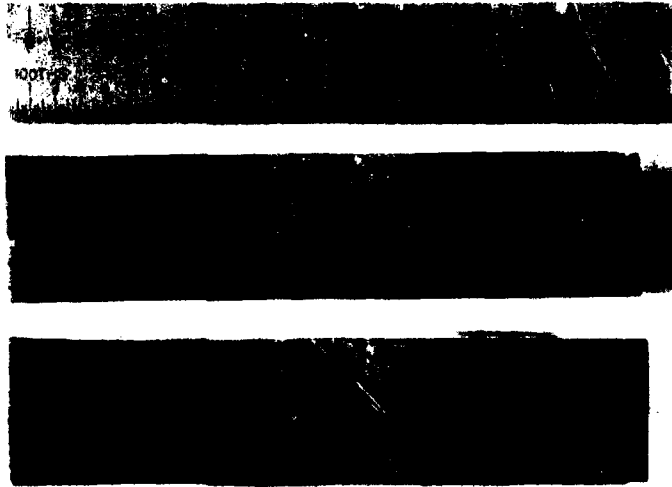


FIGURE 42. COMPACT TENSION SPECIMEN FRACTURE SURFACES
OF CLOSED DIE FORGING CD5.

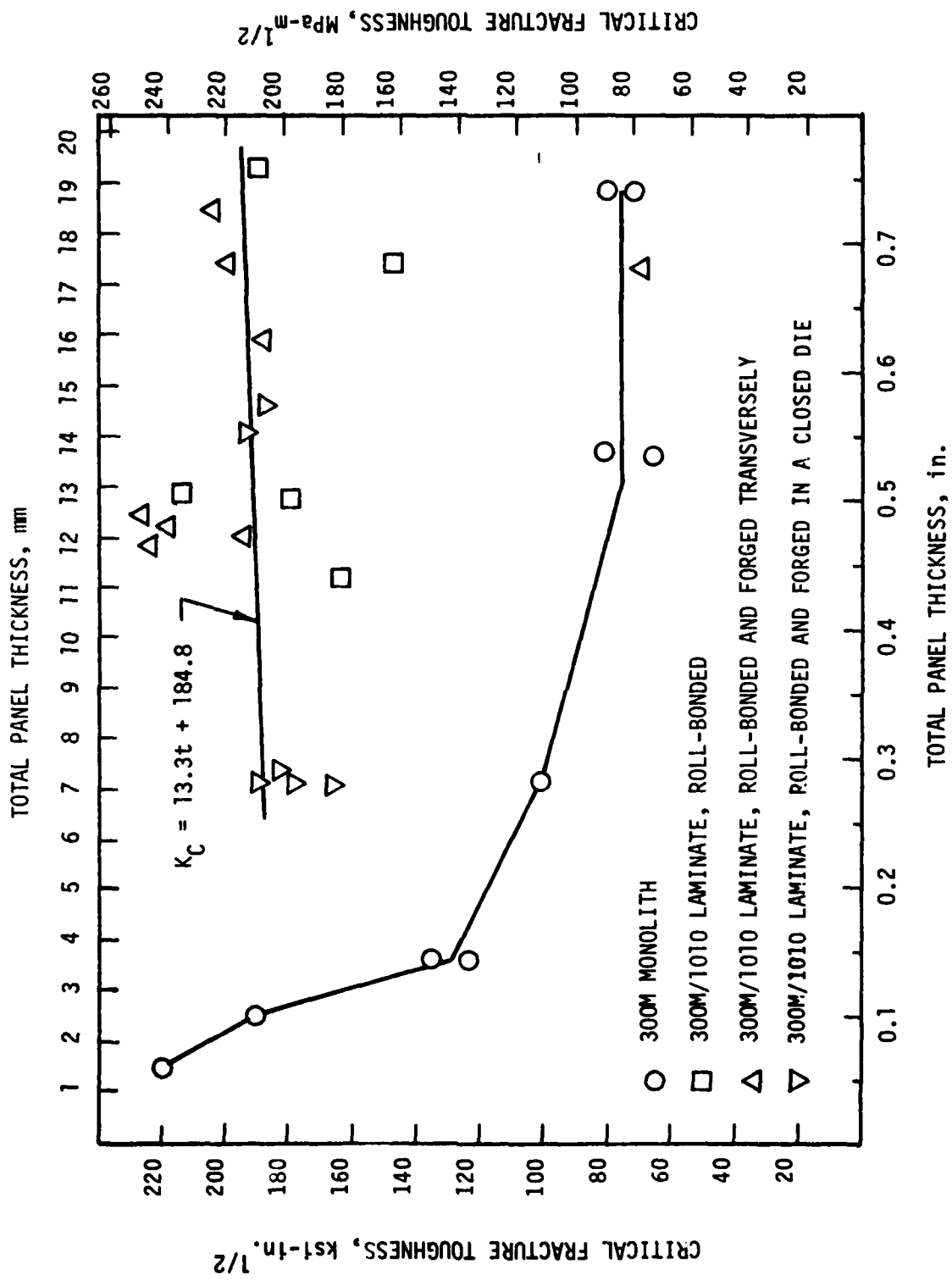


FIGURE 43. CRITICAL FRACTURE TOUGHNESS VERSUS PANEL THICKNESS FOR MONOLITHIC 300M AND THE ROLL-BONDED AND FORGED 300M/1010 LAMINATES.

critical toughness data versus layer thickness, the layer thickness of the monolithic material being tantamount to the total panel thickness, of course. This has been done in Figure 44. In general, the toughness of the laminates lies along the monolithic toughness versus thickness curve, the divergences being rationalized in terms of the bond strength and volume of low strength interleaf as discussed in Sections 3.2.3 and 3.3.3. Briefly, in review, the as roll-bonded laminate will have a slightly greater toughness than the monolithic 300M because of its low bond strength, giving rise to nearly complete layer independency, and to the energy absorbed by the low strength ductile 1010 interleaf. The forged laminates tend to have toughnesses slightly less than the monolithic material primarily is a result of the improved bond strength and somewhat more constrained mechanics, that is a shifting toward plane strain. Such a shift also explains the lower toughness of the closed die versus the transverse forgings.

The effect of stress state and elastic constraint on the toughness of laminates as compared with monolithic 300M may be deduced from the data of Figure 45 in which the conditional fracture toughness or resistance to subcritical crack growth, a linear elastic parameter is plotted versus total panel thickness. Since this fracture toughness parameter essentially represents the inception of crack advance, the metal-metal laminate property of independent layer behavior has not had the opportunity to develop and, therefore, the conditional toughness is not greatly higher than the monolithic 300M. The trend lines are determined once again by the method of least squares. It is worthy of note, however, that even the linear elastic toughness of the laminate is never lower than the monolithic plate with the exception of the one outlying point due to machine malfunction and representing essentially a dynamic fracture toughness. Furthermore, the trend line for the laminate lies everywhere above the monolithic material within the panel thickness range of plane strain monolithic toughness.

3.5 GENERAL DISCUSSION OF MATERIAL FLOW AND FRACTURE TOUGHNESS

It has been known⁵⁵ generally for some time that the proper orientation of grain flow or fiber in forgings improves mechanical integrity and toughness as a function of design and loading geometry. In particular, toughness is improved in the "cross grain" orientation in which the crack must propagate

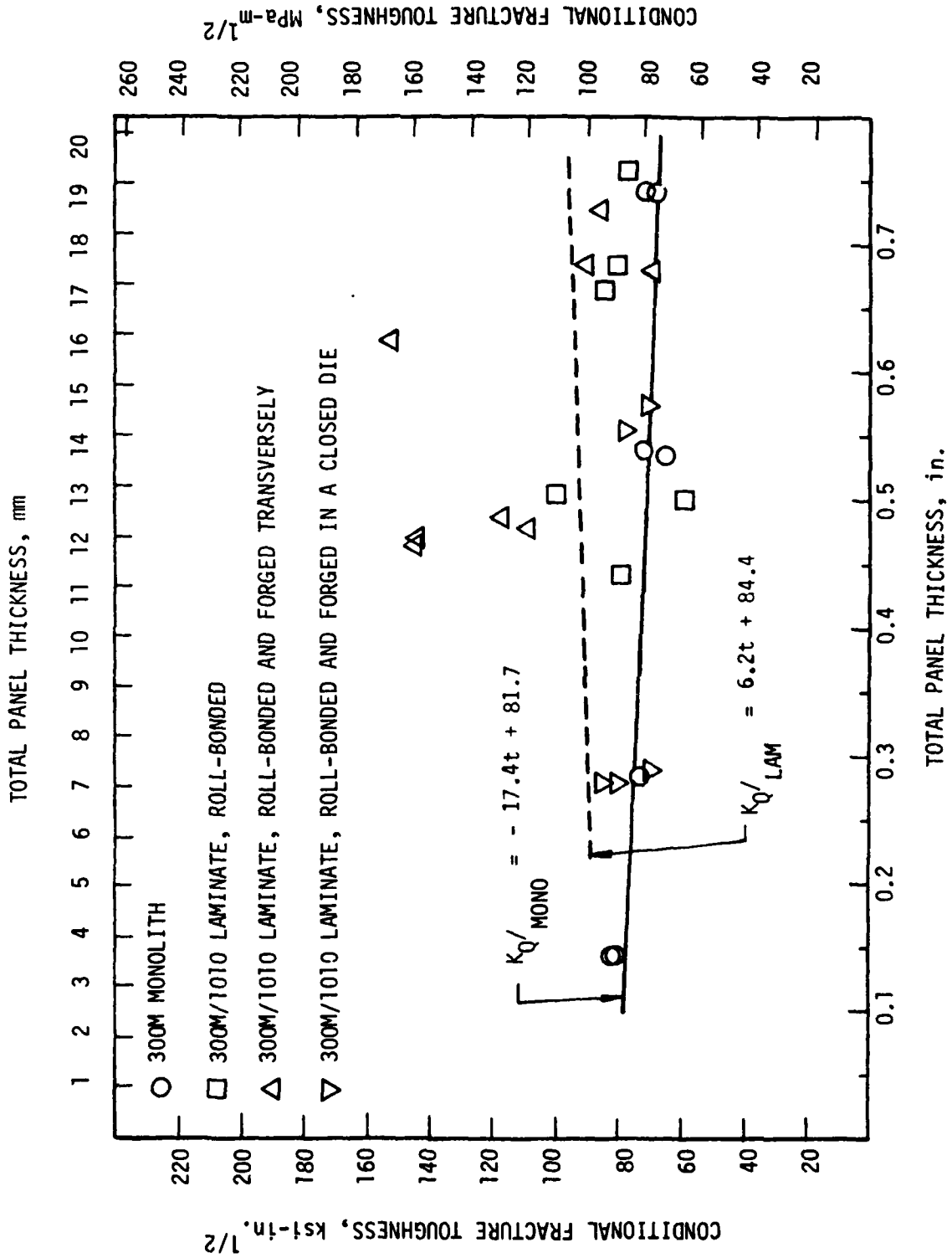


FIGURE 45. CONDITIONAL FRACTURE TOUGHNESS VERSUS PANEL THICKNESS FOR MONOLITHIC 300M AND THE ROLL-BONDED AND FORGED 300M/1010 LAMINATES.

across the fiber. The effects on toughness of both fiber or orientation and panel thickness in addition to the improvements obtainable through forging flow are shown in Figure 46. In this figure the toughness of the 4145 alloy steel used for forgeability comparison is plotted as a function of panel thickness and specimen orientation. As may be noted in the figure the improved fiber obtained through upset forging has improved the toughness vis à vis the billet for all equivalent orientations. It also is worth noting that for the 4145 both the conditional toughness, K_Q , and the critical toughness, K_C , are improved significantly by forging. Such an upsetting process for billet is a common practice within the forging industry prior to final forging of more or less tabular parts in order to fold the longitudinal fiber of the billet parallel to the forging axis for improved radial or longitudinal properties in the finished forging. The relatively high toughness of the TS orientation in the 4145 billet may seem somewhat surprising at first until it is remembered that this is a cross grain orientation and, in fact, a visual examination of the fracture surface, shown in Figure 47, will reveal a very coarse fiber representative of the billet center.

When the critical fracture toughness is plotted versus upset strain, a measure of the extent of flow, as has been done in Figure 48, the monolithic 4145 exhibits generally increasing toughness with increasing strain. This is attributable to the improved fiber of the monolithic material as discussed in the preceding paragraph. The laminate, however, with its intrinsic fiber tends to peak in toughness at the intermediate strains associated with the transversely forged laminates. The least squares trend line is still of positive slope; however, the behavior of the data may be better represented by the concave downward curve that is sketched in as well. As noted in the previous section this behavior is a consequence not of improved or worsened fiber, but rather of the change in mechanical behavior associated with both the layer thickness and the bond strength.

3.6 FATIGUE STRENGTH OF ROLL-BONDED LAMINATES

The results of the fatigue testing of as roll-bonded laminate plate and 300M monolithic plate are plotted as a Wöhler curve in Figure 49. It may be noted that the fatigue strength of the laminate is higher, in general, over

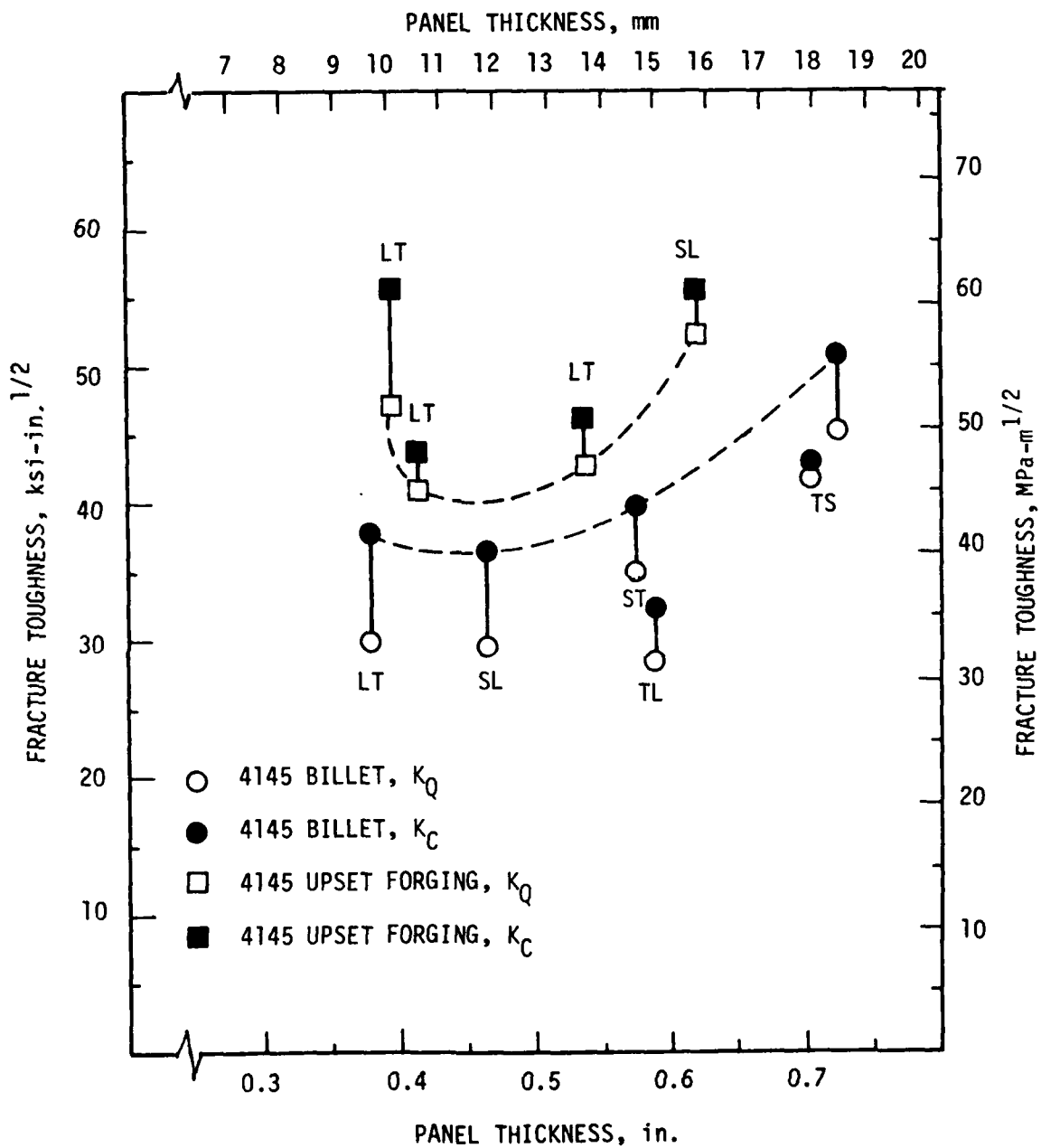


FIGURE 46. FRACTURE TOUGHNESS VERSUS PANEL THICKNESS FOR THE 4145 BILLET AND UPSET FORGINGS.

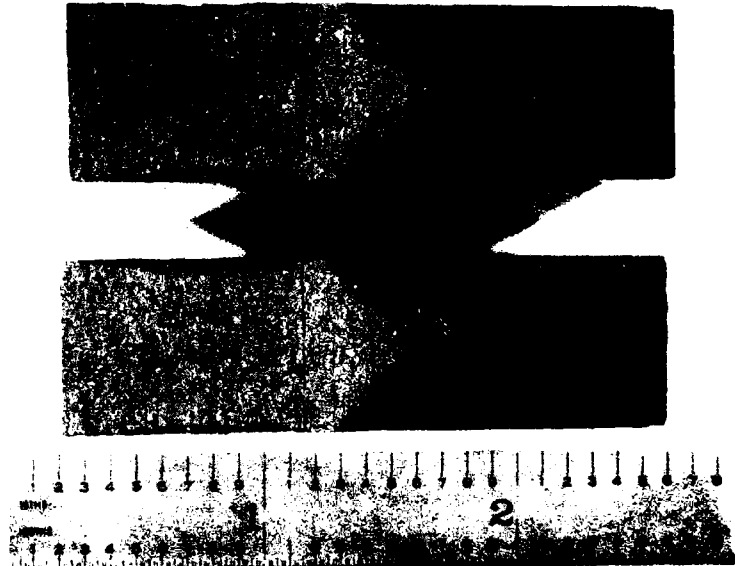


FIGURE 47. COMPACT TENSION SPECIMEN FRACTURE SURFACES
OF 4145 BILLET, TS ORIENTATION.

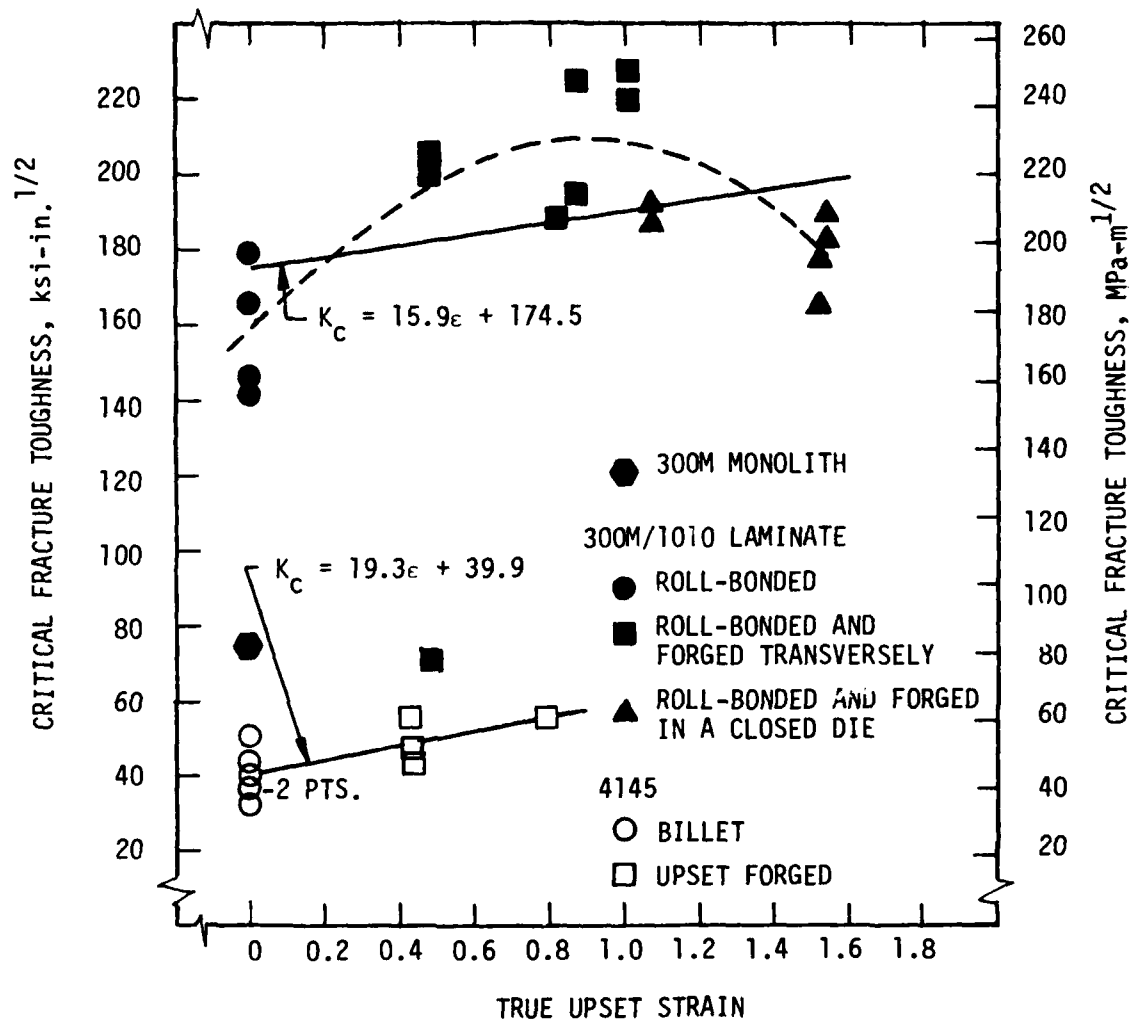


FIGURE 48. CRITICAL FRACTURE TOUGHNESS VERSUS UPSET STRAIN FOR THE 4145 AND 300M MONOLITHIC MATERIALS AND THE 300M/1010 LAMINATE.

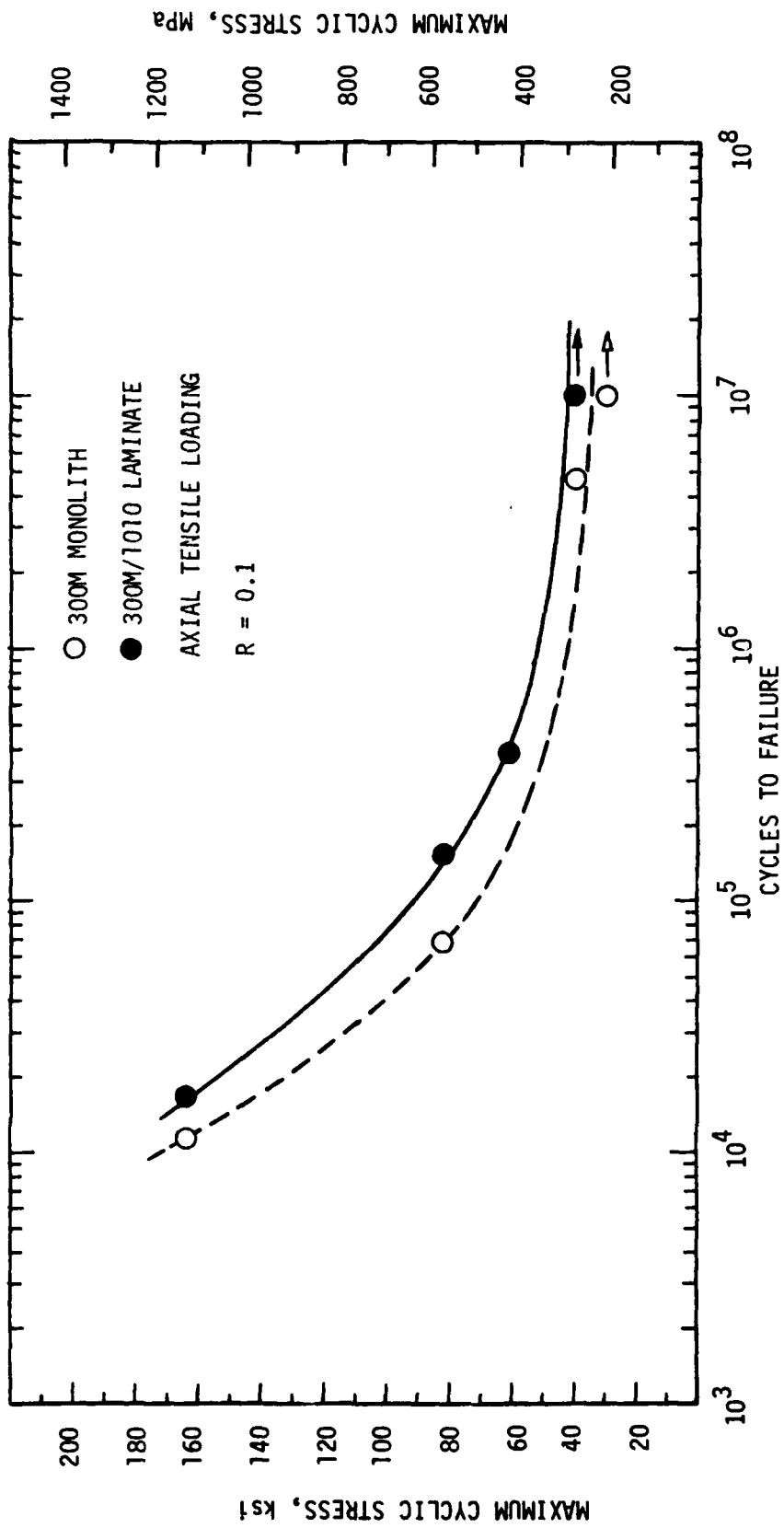


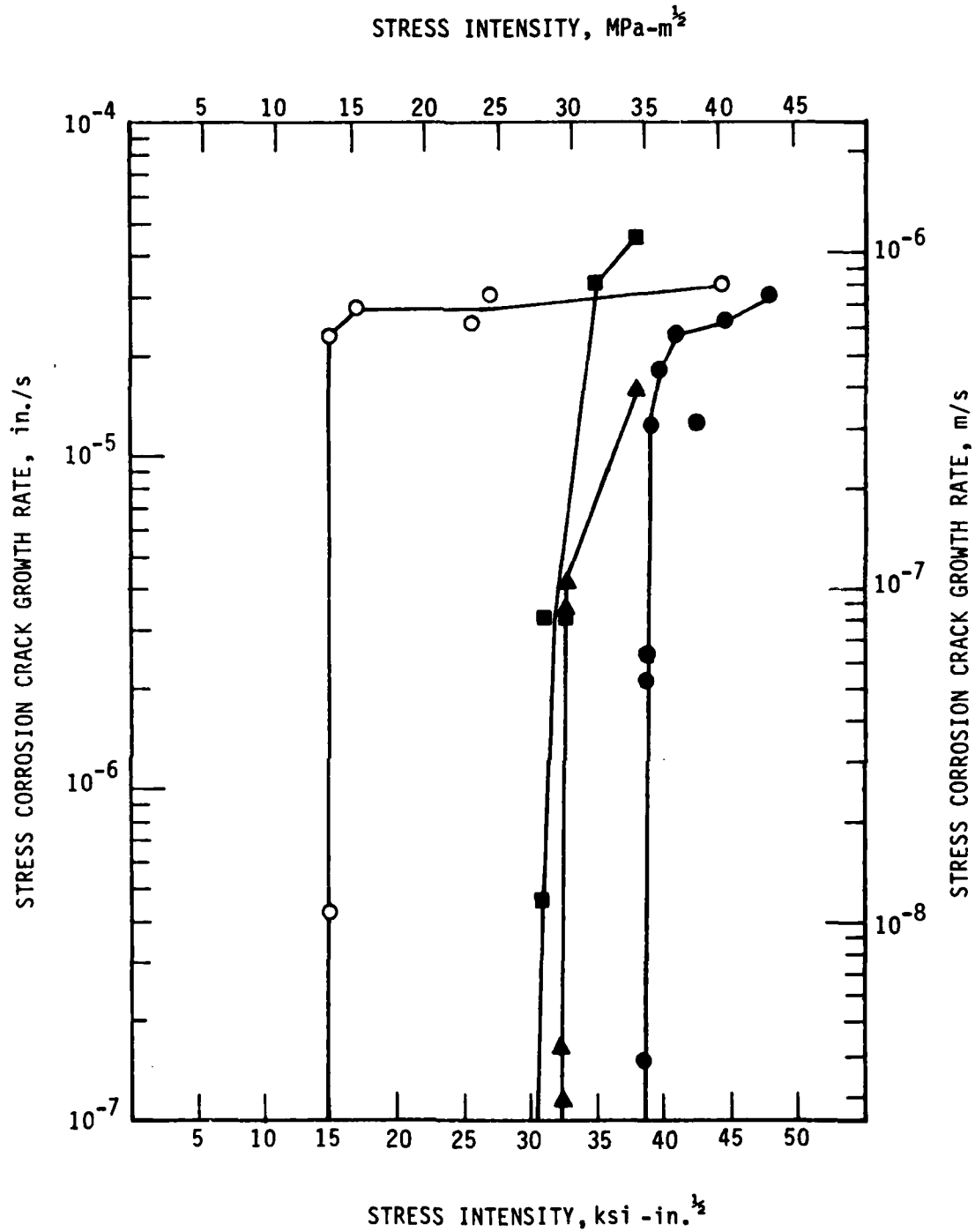
FIGURE 49. STRESS VERSUS CYCLES TO FAILURE FOR 300M MONOLITHIC PLATE AND 300M/1010 AS ROLL-BONDED LAMINATE.

the entire range examined, although it is difficult to determine if any significant improvement in the fatigue limit is obtained. Nevertheless, based on the relatively few data collected there does appear to be a significant improvement in fatigue strength at the higher stress levels. This improvement appears to stem primarily from the improved flaw tolerance of the laminate plate, such that final fast fracture of the laminate fatigue specimens was delayed even after the nucleation and subcritical growth of a crack in one layer. This flaw tolerance is primarily dependent on the crack arresting properties of the soft interleaf, although the improved fracture resistance in the crack divider orientation may contribute as well.

3.7 STRESS-CORROSION CRACKING OF ROLL-BONDED LAMINATES

The results of the stress-corrosion cracking evaluation are presented in graphical form in Figure 50. Two primary conclusions may be drawn from these data as follows: (1) The crack propagation rate at high stress intensities does not appear to differ significantly between the laminate and monolithic specimens in the crack divider orientation and (2) The threshold or critical stress intensity factor for stress-corrosion cracking, is significantly higher for the laminate material. The actual lower measured values for stress-corrosion cracking were 39.1, 33.6, and 32.3 $\text{ksi-in}^{1/2}$ (43.0, 36.9, and 35.5 $\text{MPa-m}^{1/2}$) for the laminates and 14.9 $\text{ksi-in}^{1/2}$ (16.4 $\text{MPa-m}^{1/2}$) for the monolithic 300M. These values may be taken conservatively to represent K_{Isc} . The propagation rate and K_{Isc} results for the 300M also agree well with those reported in The Damage Tolerant Design Handbook⁵⁶, which lists a maximum rate of approximately $4.2 (10^{-5}) \text{ in./s}$ ($1.06(10^{-6}) \text{ m/s}$) and a K_{Isc} of 15 $\text{ksi-in}^{1/2}$ (17 $\text{MPa-m}^{1/2}$) for 300M of similar yield strength and heat treatment and tested in a 3.5 percent sodium chloride aqueous solution.

The critical stress intensity factor represents the upper bound of load for a flawed material in a specified environment such that no subcritical crack propagation is expected, i.e., the material is safe from stress corrosion crack advance. This in turn allows a usable strength to be specified for an unprotected material in an environment of interest. The above noted results, then, permit the inference that the laminate has a usable unprotected strength greater than twice that of monolithic 300M in the test environment.



300M STEEL

○ LT ORIENTATION, 3.5% NaCl, 74°F (23.3°C)

300M/1010 LAMINATE, CRACK DIVIDER ORIENTATION

● 3 LAYER, 3% NaCl, 74°F (23.3°C)

■ 4 LAYER, 3.5% NaCl, 74°F (23.3°C)

▲ 4 LAYER, 3.5% NaCl, 74°F (23.3°C)

AVERAGE

LAYER

THICKNESS:

0.125 in. (3.18 mm)

FIGURE 50. STRESS INTENSITY VERSUS STRESS CORROSION CRACK GROWTH RATE FOR 300M STEEL (235 ksi (1620 MPa) YIELD STRENGTH) AND 300M/1010 LAMINATE (201 ksi (1386 MPa) YIELD STRENGTH). SELF-LOADED COMPACT TENSION SPECIMENS, LT ORIENTATION.

In a protected condition the laminate would be considered to have, at least, a better intrinsic factor of safety with respect to stress corrosion crack advance. In addition, the improved toughness of these laminates would require a longer flaw for catastrophic failure without regard to the cause of the flaw. As mentioned above these results and conclusions pertain to the crack divider orientation. It is also expected that the crack arresting properties of the soft interleaf would be highly effective in retarding stress-corrosion crack advance. Unfortunately, experimental difficulties encountered in precracking the bolt loaded crack arrest orientation compact tension specimens precluded the collection of stress-corrosion-cracking data in that orientation. At the time of this discovery insufficient material was available for the fabrication of bend or cantilever beam specimens for testing.

The efficacy of the metal-metal laminate system examined in improving the stress-corrosion cracking resistance of an ultrahigh strength alloy steel is demonstrated very effectively by the data of Figure 50. The important determinants of this improved behavior, however, are incompletely known or incompletely understood. Several observations of the stress-corrosion fracture surfaces can help at least to rationalize the cracking behavior of the laminate. First, as may be noted in Figure 51 the stress-corrosion crack front, which is approximately one-half inch from the end (left side) of the specimen, is convex within each individual layer indicative of crack pinning or retardation by the interleaf or layer-interleaf interface. Second, although it is difficult to distinguish reflectivities in Figure 51, the 1010 interleaf fractures are shiny and not dull and covered with corrosion product as are the 300M layer stress-corrosion fracture surfaces. From these observations it is inferred that in the crack divider orientation the interleaf and its attendant interfaces acts to pin the advancing crack, bowing it and slowing or preventing its progress, by primarily a mechanical mechanism. Since the 1010 is not as susceptible to stress-corrosion cracking as the 300M, it pins the crack until sufficient tunneling occurs and the 1010 fails by tearing. This tunneling also effectively blunts and broadens the stress-corrosion crack front. Furthermore, there appears to be an electrochemical interaction that occurs between the 1010 interleaf and 300M layer, and, based on the appearance of the two materials, the 1010 is cathodic. Although the crack dividing and primary action of the interleaves may provide some increase in the critical stress intensity through purely mechanical means, it is difficult to rationalize the

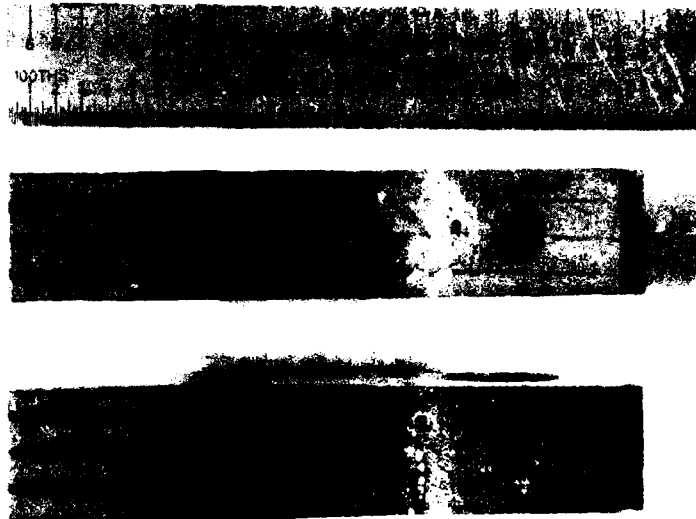
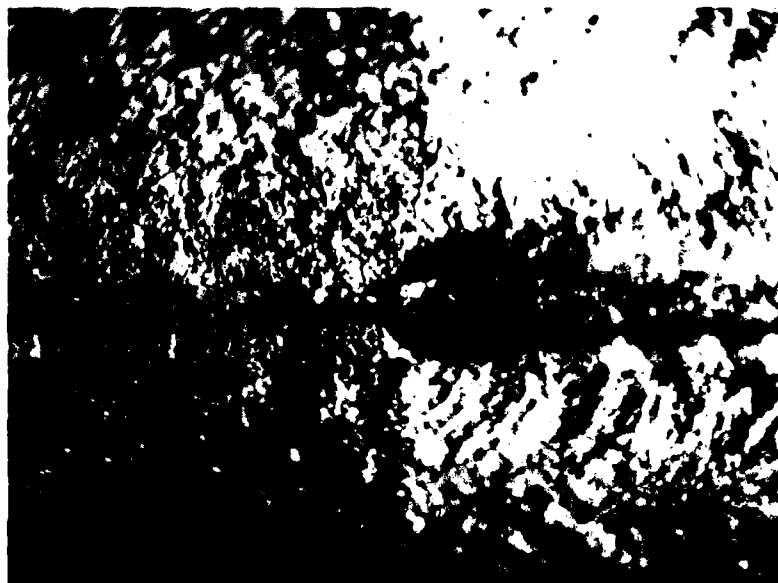


FIGURE 51. FRACTURE SURFACES OF 300M/1010 LAMINATE STRESS-CORROSION SPECIMEN TESTED IN AQUEOUS 3.5% SODIUM CHLORIDE SOLUTION AT ROOM TEMPERATURE.



1 mm

FIGURE 52. OPTICAL FRACTOGRAPH OF A STRESS-CORROSION CRACKING (SCC) SPECIMEN SHOWING THE ARRESTED STRESS-CORROSION CRACK ON THE LEFT AND FAST FRACTURE SURFACE ON THE RIGHT. MAGNIFICATION: 34X.

improvement in mechanical terms alone. An electrochemical explanation can be advanced, however, that includes both a mechanical and chemical aspect and is based primarily only on the cathodic relationship of the interleaf to the layer. Figure 52 reproduces a photograph of the arrested stress corrosion specimen and may assist in the proposed explanation. The limit of crack advance is marked by the relatively flat region at the left of the fractography. Shear lips are developed during fast fracture when the specimen was separated after cooling to the temperature of liquid nitrogen in order to expose the fracture surfaces for observation. These shear lips begin essentially at the point of stress corrosion crack advance. Since the 300M layer crack tip is anodic, it should be losing material at a rate much faster than that usually associated with stress-corrosion cracking. It is believed that this leads to significant blunting of the crack tip and provides a significant decrease in the effective stress intensity, a mechanical effect. The electrochemistry of the laminate geometry also can interfere with the mechanism of stress-corrosion cracking itself by altering the hydrogen concentration at the crack tip. It is believed that this is accomplished by the removal of the cathodic reaction, either the decomposition of water or the reduction of hydrogen, and its concomitant molecular hydrogen or gaseous hydrogen from the crack tips to the entire area of reacting interleaf, thereby decreasing the driving force for hydrogen cracking at the crack tip. Finally, two additional circumstances may also lead to lessened corrosion at the crack tip. First, the cathode to anode area ratio is small assuming that most of the exposed 300M layer surface remains active. Second, the 300M and especially the crack tip actually may become anodically passivated by reason of the galvanic corrosion. It should be noted that with the exception of some visible crack blunting at the stress-corrosion crack tip the electrochemical arguments advanced above are speculative, albeit plausible, and that their confirmation would require further experimentation and analysis of the electromechanical behavior of metal-metal laminates.

4.0 CONCLUSIONS

The present study has demonstrated and documented the feasibility of forming complex component geometries from roll-bonded steel metal-metal laminate plate stock by forging. In addition, it has been shown that the particular laminate system studied composed of layers of 300M alloy steel separated by interleaves of 1010 mild steel has distinctly improved fracture toughness, fatigue strength, and, especially, stress-corrosion cracking resistance when compared to monolithic 300M steel.

Specifically, the following conclusions are justified:

- Roll bonding of steel alloys at high temperatures is an effective and efficient process for fabricating thick multilayer laminates.
- Steel metal-metal laminates have limited but finite forgeability in the longitudinal direction and excellent forgeability in the transverse direction. The primary failure mechanism limiting formability in the longitudinal direction is hot buckling.
- In the forging of complex geometries from metal-metal laminates the die design and lubrication are critical variables for successful forming.
- The tensile properties of laminates are controlled primarily by the strength and volume fraction of the two component materials and secondarily by the strength of the inter-material interface and the relative laminal thicknesses.
- Laminate fracture toughness and, in particular, the elastic-plastic toughness or maximum resistance to critical crack growth is very much superior to corresponding monolithic material in thick section.

- The improvement in laminate fracture toughness is primarily dependent on the mechanical state of the laminate and the maintenance of a plane stress or a mixed mode stress state during fast fracture. This is predominately a function of layer thickness and the ability of the layers to decouple on fracturing, i.e., on the interleaf-layer bond strength and interleaf plastic properties.
- There is an optimum value of bond strength for maximum fracture toughness.
- The intrinsic fiber of metal-metal laminates provides a unique opportunity for controlling the directional properties of forgings using laminates as forging stock.
- The fatigue strength of steel laminates has been shown to be superior to monolithic material. This is primarily a consequence of the improved damage tolerance of the laminates.
- The stress-corrosion cracking properties of 300M/1010 laminates have been shown to be far superior to 300M steel in simulated sea water. In particular, the critical stress intensity for stress corrosion cracking is more than double that of the monolithic steel.

5.0 RECOMMENDATIONS

The results of the steel laminates properties characterization and forgeability demonstration have provided sufficient experience and confidence that a program for the fabrication of a prototype aerospace component based on steel laminates now can be initiated. Such a prototype component program would require the sinking of a die insert specifically designed for the special attributes of laminate forging, the fabrication of the component from laminate parent material, and the testing and evaluation of the component. Properly exploited the many exceptional properties of laminates, such as fracture toughness, damage tolerance, fatigue strength, and stress-corrosion cracking resistance would lead to weight savings and performance gains in aerospace items of complex shape.

It would be desirable for the fatigue and stress-corrosion cracking properties of metal-metal laminates to be characterized and analyzed more fully and in greater depth. In particular, the important parameters responsible for the exceptional stress-corrosion cracking resistance of laminates need to be defined more completely in specific service environments. This, then, would allow the design of optimum laminate systems for specific applications and the extension of stress-corrosion resistance to other alloys and environments. Such a study would provide, in addition, a novel approach for the fundamental study of the mechanisms responsible for stress corrosion cracking.

REFERENCES

1. Leslie Aitchison, A History of Metals, Interscience, New York, 1960, in two volumes, Vol. I, pp. 1-110.
2. J. R. Ellis and D. M. Hermanson, "Adhesively Bonded Multi-Layer F-104 Aft Fuselage Ring Fitting," Vought Aeronautics Co., LTV Aerospace Corp., Interim Tech. Rept. IR-843-2(1), (1972).
3. J. R. Ellis and G. E. Kuhn, "Adhesively Bonded Multi-Layer F-104 Aft Fuselage Ring Fitting," Vought Aeronautics Co., LTV Aerospace Corp., Interim Tech. Repts. IR-843-2 (2-7), (1972-1974).
4. R. D. Goolsby, "Fracture and Fatigue of Diffusion, Explosive, and Roll Bonded Al/Al and Ti/Ti Laminates," ATC Report No. B-94400/7CR-23, AD-A040 387, prepared for Naval Air Systems Command on Contract No. N00019-76-C-0288, (May, 1977).
5. S. V. Arnold, "A Laminated Specimen for Charpy Impact Testing of Sheet Metal" Proc. Am. Soc. Testing Mats., 57, 1273 (1957).
6. S. V. Arnold, "Notch Sensitivity and Resistance to Tearing of Titanium Alloy Sheet," Watertown Arsenal Laboratories, Tech. Rept. No. WAL TR 405.2/3, (1959).
7. S. V. Arnold, "Notch Sensitivity and Laminated Charpy Impact Strength of 1100-F and 2024-T6 Aluminum Alloy Simulated Sheet," Watertown Arsenal Laboratories, Tech. Rept. No. WAL TR 341.5/1, (1959).
8. S. V. Arnold, "Toughness of Steel Sheet: The Advantage of Laminating," Watertown Arsenal Laboratories, Tech. Rept. No. WAL TR 843.21/2, (1960).
9. J. L. Bluhm, "A Model for the Effect of Thickness on Fracture Toughness Applied to Laminated Structure," Proc. Am. Soc. Testing Mats. 61, 1332 (1961).

10. H. L. Leichter, "Impact Fracture Toughness and Other Properties of Brazed Metallic Laminates," J. Spacecraft, 7(3), 1113 (1966).
11. J. D. Embury, N. J. Petch, A. E. Wraith, and E. S. Wright, "The Fracture of Mild Steel Laminates," Trans. AIME, 239, 114 (1967).
12. J. G. Kaufman, "Fracture Toughness of 7075-T6 and -T651 Sheet, Plate, and Multilayered Adhesive-Bonded Panels," J. Basic Eng., Trans. ASME, 89, Series D (3), 503 (1967).
13. R. F. McCartney, R. C. Richard, and P.S. Trozzo, "Fracture Behavior of Ultrahigh-Strength-Steel Laminar Composites," Trans. ASM, 60, 394 (1967).
14. E. A. Almond, N. J. Petch, A. E. Wraith, and E.S. Wright, "The Fracture of Pressurized Laminated Cylinders", J. Iron Steel Inst., 207, 1319 (1969).
15. E. A. Almond, J. D. Embury, and E.S. Wright, "Fracture in Laminated Materials," Interfaces in Composites, ASTM STP 452, American Society for Testing and Materials, Philadelphia, Pennsylvania, 1969, p. 107.
16. S. D. Antolovich, E. Kasi, and G. R. Chanani, "Fracture Toughness of Duplex Structures: Part II - Laminates in the Divider Orientation," Fracture Toughness, Proceedings of the 1979 National Symposium on Fracture Mechanics, Part II, ASTM STP 514, American Society for Testing and Materials, Philadelphia, Pennsylvania, 1972, P. 1354.
17. S. D. Antolovich, G. R. Chanani, A. Saxena, and I. C. Wang, "Fracture Mechanism Transitions in Laminate Composites," J. Phys. D: Appl. Phys., 6, 560 (1973).
18. E. B. Kula, A. A. Anctil, and H. H. Johnson, "Fatigue Crack Growth in Dual-Hardness Steel Armor," Army Materials and Mechanics Research Center Technical Rept. AMMRC TR 74-6, (1974).
19. N. G. Ohlson, "Fracture Toughness of Laminated Steel," Eng. Fract. Mech., 6 (3), 459 (1974).

20. T. M. Devine, S. F. Floreen, and H. W. Hayden, "Fracture Mechanisms in Maraging Steel-Iron Laminates," Eng. Fract. Mech., 6 (2), 315 (1974).
21. D. Cox and A. S. Tetelman, Improved Fracture Toughness of Ti-6Al-4V Through Controlled Diffusion Bonding, Air Force Materials Laboratory Technical Rept. AFML-TR-71-264, (1972).
22. D. O. Cox and A. S. Tetelman, Fracture Toughness and Fatigue Properties of Titanium Laminate Composites Produced by Controlled Diffusion Bonding, Air Force Materials Laboratory Technical Rept. AFML-TR-73-288 (1973).
23. S. Floreen, N. Kenyon, and H. W. Hayden, "The Fabricability and Toughness of Laminar Composites of Maraging Steel", Trans. ASME, J. Engr. Mater. Tech., Vol. 96, Series H (3), 176 (1974).
24. J. F. Throop and J. J. Miller, "Fatigue Behavior of Metal Laminates", AD 785 690, Army Science Conference Proceedings, Vol. III, AD 785 672, 229 (1974).
25. J. A. Alic, "Stable Crack Growth in Adhesively Bonded Aluminum Alloy Laminates," Internal J. Fracture ,11 (4), 701 (1975).
26. H. W. Hayden and S. Floreen, "The Deformation and Fracture of Stainless Steel Having Microduplex Structures", Trans. ASM, 61, 474 (1968).
27. S. Floreen, H. W. Hayden, and R. M. Pilliar, "Fracture Behavior of an Fe-Cu Microduplex Alloy and Fe-Cu Composites," Trans. AIME, 245, 2529 (1969).
28. S. Floreen, H. W. Hayden, and J. Q. Steigelman, "Fracture Modes in Laminated Steel Nickel Composites," Trans. ASM, 62, 812 (1969).
29. J. Cook and J. E. Gordon, "A Mechanism for the Control of Crack Propagation in All-Brittle Systems," Proc. Roy. Soc. (London), 282A, 508-520 (1964).

30. J. D. Embery, N. J. Petch, A. E. Wraith, and E. S. Wright, "The Fracture of Mild Steel Laminates," Met. Trans, 239, 114-118 (1967).
31. J. F. Throop and J. J. Miller, "Fatigue Behavior of Metal Laminates," WVT-TR-75035, Watervliet Arsenal, June 1975.
32. J. F. Throop and R. R. Fuczak, "Fracture Resistant Titanium-Aluminum Laminate," in Toughness and Fracture Behavior of Titanium, ASTM STP 651, American Society for Testing and Materials, Philadelphia, Pennsylvania, 1978, pp. 246-266.
33. R. M. Johnson, "Fracture and Fatigue of Diffusion, Adhesive, and Roll-Bonded Aluminum, Titanium, and Ultrahigh Carbon Steel Laminates," ATC Report No. B-921C0/8CR-80, AD-A058 553, Prepared for Naval Air Systems Command on Contract No. N00019-77-C-0287, Vought Corporation, Advanced Technology Center, May 1978.
34. R. M. Johnson and R. D. Goolsby, "Diffusion, Roll and Explosive Bonding of Al/Al, Ti/Al, and Ti/Ti Laminates," in MATERIALS SYNERGISMS, 10TH National SAMPE Tech. Conf., Society for the Advancement of Material and Process Engineering, 1978, pp. 802-811.
35. L. E. Slotter and D. H. Petersen, "Fatigue and Fracture of Ultrahigh Strength Steel and Titanium Roll-Bonded and Diffusion-Bonded Laminates," ATC Report No. R-92000/OCR-31, prepared for Naval Air Systems Command on Contract No. N00019-78-C-0491, AD-A086 511/3, Vought Corporation, Advanced Technology Center, May 1980.
36. L. E. Slotter and D. H. Petersen, "Fracture and Fatigue of Metal-Metal Laminates," in Material and Process Applications, Land, Sea, Air, Space, 26th National SAMPE Symposium Proceedings, Vol. 26, Society for the Advancement of Material and Process Engineering, 1981, pp. 313-324.
37. "Standard Method of Test for Plane-Strain Fracture Toughness of Metallic Materials," ASTM E 399-81, American Society for Testing and Materials, Philadelphia, Pennsylvania, 1981.

AD-A127 541

ROLL-BONDED 300M/1010 STEEL METAL-METAL LAMINATES:
FORGEABILITY TOUGHNESS..(U) VOUGHT CORP ADVANCED
TECHNOLOGY CENTER DALLAS TX L E SLOTER JUN 82

2/2

UNCLASSIFIED

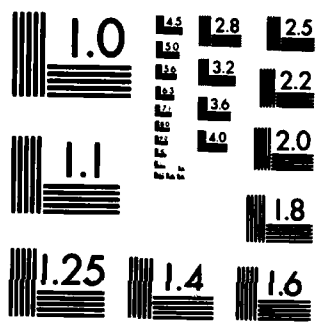
ATC-R-92000/2CR-20 N00019-80-C-0575

F/G 11/6

NL



END
DATE
FILMED
583
DFIC



MICROCOPY RESOLUTION TEST CHART
NATIONAL BUREAU OF STANDARDS-1963-A

38. "Military Specification: Steel Bars, Reforging Stock, and Mechanical Tubing Low Alloy, Premium Quality," MIL-S-8844C, 25 May 1971.
39. J. E. Jenson (ed.), Forging Industry Handbook, Forging Industry Association, Cleveland, Ohio, pp. 193-194.
40. Alloy Digest, Engineering Alloys Digest, Inc., Upper Montclair, New Jersey.
41. Metals Handbook, Ninth Edition, Vol. 1, Properties and Selection: Irons and Steels, American Society for Metals, Metals Park, Ohio, 1978, pp. 120, 125, and 127.
42. "Standard Methods of Tension Testing of Metallic Materials," ASTM E 8-81, 1981 Annual Book of ASTM Standards, Part 10, Metals - Physical, Mechanical, Corrosion Testing, American Society for Testing and Materials, Philadelphia, Pennsylvania, 1981, pp. 197-217.
43. "Standard Test Method for Plane-Strain Fracture Toughness of Metallic Materials," ASTM E 399-81, 1981 Annual Book of ASTM Standards, Part 10, Metals-Physical, Mechanical, Corrosion Testing, American Society for Testing and Materials, Philadelphia, Pennsylvania, 1981, pp. 588-618.
44. W. A. Backofen, Deformation Processing, Addison-Wesley, Reading, Massachusetts, 1972, pp. 151-152.
45. Atlas of Isothermal Transformation and Cooling Transformation Diagrams, American Society for Metals, Metals Park, Ohio, 1977, pp. 396-397.
46. F. E. Adams, Vought Corporation, Dallas, Texas, private communication.
47. J. E. Jenson, Forging Industry Handbook, Forging Industry Association, Cleveland, Ohio, p. 106.
48. F. A. D'Isa, Mechanics of Metals, Addison-Wesley, New York, pp. 100-102.

49. F. R. Shanley "Inelastic Column Theory," J. Aero. Sci., 14(5), 261-267 (1947).
50. S. L. Semiatin and H. R. Piehler, "Deformation of Sandwich Sheet Materials in Uniaxial Tension," Met. Trans., 10A, 85-96 (1979).
51. S. L. Semiatin and H. R. Piehler, "Formability of Sandwich Sheet Materials in Plane Strain Compression and Rolling," Met. Trans., 10A, 97-107 (1979).
52. G. E. Dieter, Mechanical Metallurgy, McGraw-Hill, New York, 1961, P. 246.
53. F. A. D'Isa, Mechanics of Metals, Addison-Wesley, New York, P. 143.
54. Irwin Miller and John E. Freund, Probability and Statistics for Engineers, Prentice-Hall, Englewood Cliffs, New Jersey, 1965, pp. 226-231.
55. J. E. Jenson, Forging Industry Handbook, Forging Industry Association, Cleveland, Ohio, pp. 10-11.
56. Damage Tolerant Design Handbook, MCIC-HB-01, Metals and Ceramics Information Center, Battelle Columbus Laboratories, Columbus, Ohio, January 1975, pp. 7.2-3 (12/72) and 6.2-11(1/75).

CONTRACT DISTRIBUTION LIST

Commander
Naval Air Systems Command
Attn: J. S. Bruce (AIR-5163C6)
Washington, DC 20361

Commander
Naval Air Systems Command
Attn: Code AIR-950D
Department of the Navy
Washington, DC 20361

Commander
Department of the Navy
Naval Sea Systems Command
Attn: Code 03423 (1 copy)
Washington, DC 20361

Chief of Naval Research
Department of the Navy
Attn: Code ONR 423 (1 copy)
Code ONR 471 (1 copy)
Washington, DC 20361

Director
U. S. Naval Research Laboratory
Attn: Dr. Ray Hettche
Dr. B. B. Rath
Dr. G. Yoder
Washington, DC 20390

Commander
Naval Air Development Center
Attn: Code 606
Warminster, PA 18974

Commanding Officer
Naval Air Rework Facility
Naval Air Station, Bldg 604
Attn: Code 34100
Pensacola, FL 32508

Commanding Officer
Naval Air Rework Facility
Naval Air Station, North Island
Attn: Code 34100
San Diego, CA 92135

Naval Material Industrial Resources
Philadelphia, PA 19112

Contract Distribution List (Continued)

Director
Air Force Materials Laboratory
Attn: Codes LLMO (1 copy)
 LC (1 copy)
 MXE (1 copy)
 MBC (1 copy)
 LLS (1 copy)
Wright-Patterson AFB, OH 45433

Army Aviation Systems Command
P. O. Box 209
St. Louis, MO 63166

Department of the Interior
Bureau of Mines
Washington, DC 20240

U. S. Energy Research & Development Administration
Division of Reactor R&D
Attn: Mr. J. M. Simmons (1 copy)
 Chief, Metallurgy Section
Washington, DC 20545

Battelle Memorial Institute
Defense Metals Information Center
505 King Avenue
Attn: Mr. Richard Wood (1 copy)
Columbus, OH 43201

AVCO Space Systems Division
Lowell Industrial Park
Lowell, MA 01851

Brush Wellman, Inc.
17876 St. Clair Avenue
Cleveland, OH 44110

NASA/Langley
Manufacturing Technology Section
Attn: Mr. Tom Bales (1 copy)
Hampton, VA 23365

McDonnell-Douglas Research Laboratories
P. O. Box 516
Attn: Dr. D. P. Ames (1 copy)
 Dr. C. Whitsett (1 copy)
 Mr. H. C. Turner (1 copy)
 Mr. H. J. Siegel (1 copy)
 (M&P Development Dept,
 General Engineering Div.)
St. Louis, MO 63166

The Franklin Institute Research Laboratories
Twentieth & Parkway
Attn: Technical Director (1 copy)
Philadelphia, PA 19103

Contract Distribution List (Continued)

Dr. John A. Schey (1 copy)
Department of Mechanical Engineering
University of Waterloo
Waterloo, Ontario, Canada N2L 3 G1

AIResearch Company
Materials Applications Group
93-3G1-503-4V (1 copy)
402 South 36th Street
Phoenix, AZ 85010

Wyman Gordon Company
Attn: Mr. Charles Gure (1 copy)
Worcester Street
North Crafton, MA 05163

Kawecki Berylco Industries
P. O. Box 1462
Attn: Dr. J. P. Denny (1 copy)
Reading, PA 19603

Ladish Company
Packard Avenue
Attn: Mr. Robert Daykin (1 copy)
Cudahy, WI 53110

Linde Company
Division of Union Carbide
P. O. Box 44
Tonawanda, NY 14152

Midwest Research Institute
425 Volker Boulevard
Kansas City, MO 64110

Nuclear Metals, Incorporated
Attn: Dr. Paul Lowenstein (1 copy)
2229 Main Street
Concord, MA 01742

General Electric
Missile & Space Division
Materials Science Section
Attn: Technical Library (1 copy)
P. O. Box 8555
Philadelphia, PA 91901

Reynolds Metals Company
Reynolds Metals Building
Attn: Technical Library (1 copy)
Richmond, VA 23218

Contract Distribution List (Continued)

Artech Corporation
2816 Fallfax Drive
Attn: Mr. Henry Hahn (1 copy)
Falls Church, VA 22042

LTV Aerospace Corporation
SPVR, Engineering Materials
Vought Systems Division
Attn: Mr. A. E. Hohman, Jr. (1 copy)
P. O. Box 5907
Dallas, TX 75222

Advanced Technology Center, Inc.
Attn: Dr. D. H. Peterson (1 copy)
(Senior Scientist)
P. O. Box 6144
Dallas, TX 75222

Defense Advanced Research Project Agency
1400 Wilson Boulevard
Attn: Dr. E. C. VanReuth (1 copy)
Arlington, VA 22209

Grumman Aerospace Company
Advanced Material & Processing Div.
Attn: Mr. Carl Micillo (1 copy)
Bethpage, LI, NY 11714

Aluminum Company of America
1200 Ring Building
Attn: Mr. G. B. Barthold (1 copy)
Washington, DC 20036

Massachusetts Institute of Technology
Dept. of Metallurgy & Material Science
Attn: Dr. N. J. Grant (1 copy)
Cambridge, MA 02139

Drexel University
Dept of Metallurgical Engineering
Attn: Dr. Alan Lawley (1 copy)
32nd & Chestnut Streets
Philadelphia, PA 19104

Reactive Metals, Incorporated
Attn: Dr. Howard Bomberger (1 copy)
Miles, OH 44446

Lockheed Aircraft
Dept. 74-50, Bldg. #85
Attn: Mr. Rod Siemens (1 copy)
Burbank, CA 91520

Contract Distribution List (Continued)

Lockheed Missiles & Space Co., Inc.
Palo Alto Research Laboratory
Attn: Dr. Thomas E. Tietz (1 copy)
(52-31/204)
3251 Hanover Street
Palo Alto, CA 94304

Rockwell International Corporation
Science Center
P. O. Box 1085
Attn: Dr. Neil Paton (1 copy)
1049 Camino Dos Rios
Thousand Oaks, CA 91360

Douglas Aircraft Company
3855 Lakewood Boulevard
Long Beach, CA 90846

Pratt & Whitney Aircraft
Division of United Aircraft Corp
Florida Research & Development Ctr
P. O. Box 2691
Attn: Mr. John Miller (1 copy)
West Palm Beach, FL 33402

Crucible Materials Research Center
P. O. Box 88
Parkway West & Route 60
Attn: Mr. E. J. Dulis (1 copy)
Pittsburgh, PA 15230

Reynolds Metals Corporation
Attn: Mr. George Hsu (1 copy)
Manager of Industry Standards
6601 West Broad Street
Richmond, VA 23261

Henry Krumb School of Mines
Columbia University
Attn: Dr. John K. Tien
New York, NY 10027

Gould, Inc.
Gould Information Center
540 East 105th Street
Cleveland, OH 44108

Commonwealth Scientific
500 Pendleton Street
Attn: Mr. A. P. Divecha (1 copy)
Alexandria, VA 22314

Contract Distribution List (Continued)

The Boeing Company
12842 - 72nd Avenue, N.E.
Attn: Mr. W. Spurr (1 copy)
Kirkland, WA 98033

Rockwell International
Columbus Division
Attn: Mr. P. Maynard (1 copy)
Dept. 75, Group 521
Columbus, OH 43216

Rockwell International
Los Angeles Division
International Airport
Attn: Gary Keller (1 copy)
(Materials Applications)
Los Angeles, CA 90009

Martin-Marietta Aerospace
New Technology - Metals
Denver Division
Attn: Mr. Geisendorfer (1 copy)
P. O. Box 179
Denver, CO 80201

Grumman Aerospace Corp
Adv. Mat. & Processes
ATTN: Mr. Bill Grant
Bethpage, LI, NY 11714

